NKS-500
ISBN 978-87-7893-598-4

NKS- Project TRIO; Tellurium, Iodine and Caesium Interactions with Boric Acid during a Nuclear Accident (2023-2024)

Fredrik Börjesson Sandén[1]
Anna-Elina Pasi[2]
Teemu Kärkelä[2]
Tuula Kajolinna[2]
Christian Ekberg[1]

[1]Chalmers University of Technology, Kemivägen 4,
SE-412 96 Gothenburg, Sweden
[2]VTT Technical Research Centre of Finland Ltd, P.O. Box 1000,
FI-02044 VTT, Espoo, Finland

April 2025

Abstract

Project TRIO was a project partially funded by NKS 2023-2024, and a joint collaboration between Chalmers University of Technology and VTT technical research institute in Finland. The project aim was to investigate if and how boric acid influences volatile fission product behaviour in severe nuclear accident-like conditions, with a special focus on tellurium. The project was split into two parts, with the first one investigating the influence of just tellurium and boric acid, and the other one also including vaporized Iodine, as well as caesium iodide. The experiments involved volatilization of tellurium into a carrier gas, into which boric acid solution was added. This yielded filters and liquid traps which were analysed, chiefly with ICP-MS and XPS and SEM-EDX. Online aerosol measurements (TEOM and ELPI) were also used.
The results imply that there is little direct interaction between tellurium and boric acid, as the Te-B chemical bond is never detected. However, boric acid decreases the tendency for tellurium to oxidize, and it is part of an interaction involving tellurium, iodine and boric acid all together which results in an increase in tellurium volatility by several orders of magnitude.

Key words

Severe Nuclear Accidents, Tellurium, Iodine, Fission Products, Boric Acid

NKS-500
ISBN 978-87-7893-598-4
Electronic report, April 2025
NKS Secretariat
P.O. Box 49
DK - 4000 Roskilde, Denmark
Phone +45 4677 4041
www.nks.org
e-mail nks@nks.org

NKS- Project TRIO; Tellurium, Iodine and Caesium Interactions with Boric Acid during a Nuclear Accident (2023-2024)

Final Report from the NKS-R TRIO-activity

(Contract: AFT/NKS-R(23)139/6)

Fredrik Börjesson Sandén[1]
Anna-Elina Pasi[2]
Teemu Kärkelä[2]
Tuula Kajolinna[2]
Christian Ekberg[1]

[1]Chalmers University of Technology, Kemivägen 4, SE-412 96 Gothenburg, Sweden
[2]VTT Technical Research Centre of Finland Ltd, P.O. Box 1000, FI-02044 VTT, Espoo, Finland

Abstract

Project TRIO was a project partially funded by NKS 2023-2024, and a joint collaboration between Chalmers University of Technology and VTT Technical Research Centre of Finland. The project aim was to investigate if and how boric acid influences volatile fission product behaviour in severe nuclear accident-like conditions, with a special focus on tellurium. The project was split into two parts, with the first one investigating the influence of just tellurium and boric acid, and the other one also including vaporized iodine, as well as caesium iodide. The experiments involved volatilization of tellurium into a carrier gas, into which boric acid solution was sprayed. The resulting gas-aerosol mixture was directed through a filter and a liquid trap which were analysed using XPS and SEM-EDX, and ICP-MS respectively. Online measurements (TEOM and ELPI) of the aerosol characteristics were also used.
The results imply that there is little direct interaction between tellurium and boric acid, as the Te-B chemical bond is never detected. However, boric acid decreases the tendency for tellurium to oxidize, which may affect the volatility of tellurium species in an accident. Furthermore, when tellurium, iodine and boric acid all are present together, there is an increase in tellurium volatility by several orders of magnitude, compared to if either component is missing.

Contents

1. Introduction

Project TRIO was conceived to start investigating the influence of boric acid on the transport of fission products in situations simulating a severe accident.
Fission products occur due to the fission of nuclear fuel in the reactor, and are almost invariably radioactive; in fact, they are responsible for the large increase in radioactivity of spent fuel compared to fresh fuel. Fission products encompass a large span of the periodic table, and so the chemical behaviour of them is highly variable. However, certain fission products are of greater interest than others due to their chemical, biological, or radiological characteristics. Among the most interesting are the volatile fission products iodine, caesium and tellurium[1].
Iodine is a halogen which boils at 184 ^{o}C at standard pressure. Radioactive iodine is of great concern in case of a nuclear accident as it has a biological role and is stored in the thyroid gland in mammals, including humans. Radioactive iodine is thus taken up and concentrated to the thyroid gland, giving a prolonged, localized dose of radiation which may cause cancer later in life [2].
Caesium is an alkali-metal and highly reactive chemically. It only exists in the form of cations in nature, and the same is true in the case of nuclear accidents. It has been found alongside iodine (CsI, an aerosol) as well as several other anionic species, such as various metal oxides (e.g. Cs_2MoO_4, or $CsBO_2$)[3]. Interaction with tellurium is also potentially possible [4].
Caesium is also radiologically important since ^{137}Cs has a long half-life of 31.7 years, making caesium contamination a long-lasting environmental concern. Other radiologically important caesium isotopes include ^{134}Cs (half-life 2.1 years) and ^{136}Cs (half-life 13.2 days).
Tellurium is a metalloid with a variable chemistry as it can readily become oxidated at higher oxygen partial pressures and high temperature [5]. It can also interact with hydrogen to form the volatile, toxic gas of hydrogen telluride, though this species is not stabile at ambient temperatures. Tellurium can also, much like iodine, interact with organic species to form organic tellurides; a reaction of interest in nuclear accident scenarios [6]. These species are highly volatile, with boiling points around 100 ^{o}C. This can be compared to metallic tellurium, which boils at 990 ^{o}C.
Severe accidents are complex phenomena, involving the fission products, structural material such as steel and concrete, zircalloy cladding as well as paints and cables. Furthermore, the accident response measures further change the picture. Water is typically pH-adjusted to be alkaline to prevent iodine from volatizing from the water. Furthermore, boric acid is a popular additive due to the neutron absorbing capabilities of ^{10}B. This makes boric acid a very likely species to be included in the accident chemistry, and its effects on the chemistry warrants investigating.

The TRIO project resulted in two papers. The first one is published under open access in "Annals of Nuclear energy": F. Börjesson Sandén, T. Kärkelä, A-E. Pasi, T. Kajolinna, C. Ekberg, *Effects of boric acid on volatile tellurium in severe accident conditions*, *Annals of nuclear energy*, vol 200, 2024.
The second paper accepted for publication under open access in "Nuclear Technology":
F. Börjesson Sandén, T. Kärkelä, A-E. Pasi, T. Kajolinna, C. Ekberg, *Effect of Boric Acid on Volatile Fission Products in Conditions Simulating a Severe Nuclear Accident*
Both papers are attached as appendices.

2. Experiments and Method

Two sets of experiments were conducted (each set corresponding to one of the two papers published). The first set is described in Table 1, and the other one in Table 2.

Table 1. Experiments conducted to investigate the effect of boric acid on tellurium volatility.

Experiment designation	Temperature[ºC]	Atmosphere	Injection
Ref_Ox_LT	300	Oxidizing (Air)	-
Exp_Ox_LT	300	Oxidizing (Air)	$B(OH)_3$ (aq)
Ref_Ox_HT	650	Oxidizing (Air)	-
Exp_Ox_HT	650	Oxidizing (Air)	$B(OH)_3$ (aq)
Ref_In_LT	300	Inert (N_2)	-
Exp_In_LT	300	Inert (N_2)	$B(OH)_3$ (aq)
Ref_In_HT	650	Inert (N_2)	-
Exp_In_HT	650	Inert (N_2)	$B(OH)_3$ (aq)
Ref_Rd_LT	300	Reducing (H_2/Ar)	-
Exp_Rd_LT	300	Reducing (H_2/Ar)	$B(OH)_3$ (aq)
Ref_Rd_HT	650	Reducing (H_2/Ar)	-
Exp_Rd_HT	650	Reducing (H_2/Ar)	$B(OH)_3$ (aq)

Table 1 contains the experimental plan that forms the basis for the paper "*Effects of boric acid on volatile tellurium in severe accident conditions*" and these experiments are henceforth collectively referred to as "Series 1". The experiments aim to investigate how the volatility of tellurium changes due to the presence of boric acid in different atmospheres and temperatures. The experiments were conducted over two temperatures (300 and 650 ºC), and in three different atmospheres (synthetic air, N_2, and 5% H_2 in Ar). For each temperature and atmosphere, there is one "reference condition," without $B(OH)_3$, followed by the same temperature and atmosphere which includes $B(OH)_3$.

Table 2 contains the experimental plan for the paper "*Effect of Boric Acid on Volatile Fission Products in Conditions Simulating a Severe Nuclear Accident*". In principle, the plan mirrors the one presented in Table 1 making use of the same atmospheres. However, the experimental matrix and setup had to be altered to accommodate for the expanded range of fission products, now including iodine and caesium. These experiments will collectively be referred to as "Series 2".

In Series 1, the interaction with boric acid and tellurium alone is studied. Series 2 expands this to also include iodine together with tellurium, and iodine together with tellurium and boric acid. In addition, one experiment in each atmosphere was conducted using CsI as the source of iodine and caesium.

Table 2. Experiments conducted to investigate the effect of boric acid on tellurium in the presence of iodine and Caesium iodine.

Experiment	Atmosphere	Injected through atomizer	Fission products
1.1	Oxidizing (Air)	-	I, Te
1.2	Oxidizing (Air)	$B(OH)_3$	I, Te
1.3	Oxidizing (Air)	$B(OH)_3$, CsI	Te

2.1	Reducing (Ar/H_2)	-	I, Te
2.2	Reducing (Ar/H_2)	$B(OH)_3$	I, Te
2.3	Reducing (Ar/H_2)	$B(OH)_3$, CsI	Te
3.1	Inert (N_2)	-	I, Te
3.2	Inert (N_2)	$B(OH)_3$	I, Te
3.3	Inert (N_2)	$B(OH)_3$, CsI	Te,

3. Experiment equipment and procedure

The two experimental series (Series 1 and Series 2) use a similar setup. The schematic setup is depicted in figure 1, with the main difference between the two experimental processes being that the analytical methods TEOM (Tapared Element Oscillating Microbalance) and ELPI (Electrical Low-Pressure Impactor), which were used to characterize aerosols were disconnected for Series 2, as the iodine vapour would interfere with them. Furthermore, a system to feed iodine was put in place. These changes are depicted in Figure 1.
A detailed description of the systems can be found in the respective papers, including brands and names of the components, materials and gas flows. However, an overview of the core system and its use is presented here for context.
The sample is made up of 5 g metallic tellurium. The sample was heated to 540 °C; sufficient to cause considerable volatilization of the tellurium. The vapour is transported down the furnace together with the carrier gas. Boric acid solution (0.2 M) and CsI solution (38.5 mM) is injected through an atomizer and was carried by another stream of carrier gas. Iodine was supplied by heating solid iodine in a 65 °C water bath. The vapour was carried with the relevant atmospheric gases.

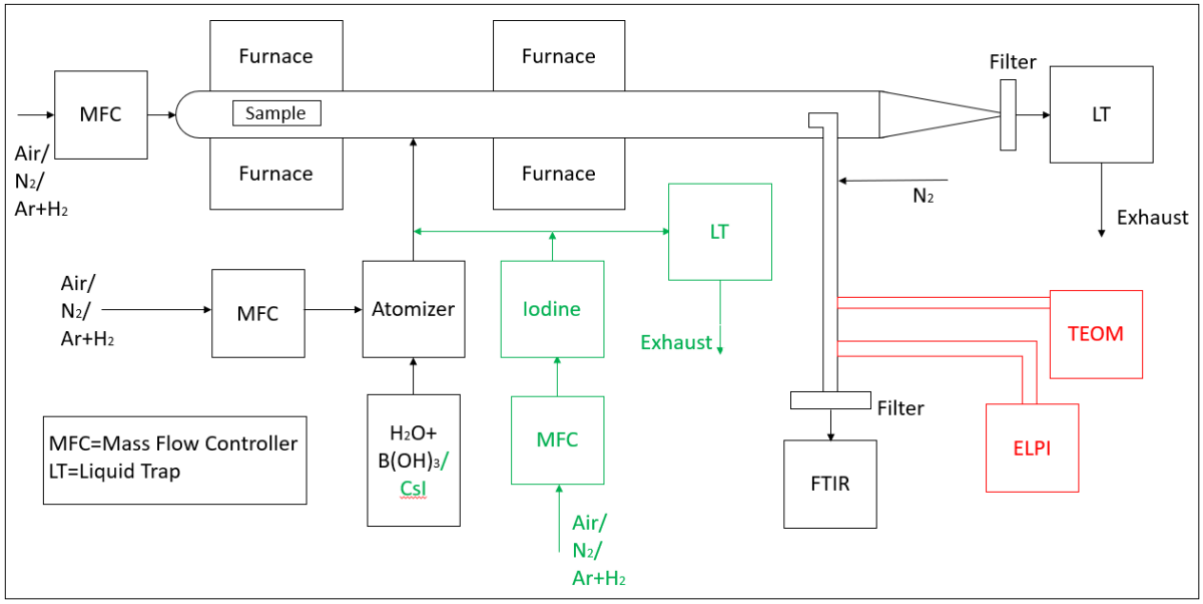

Figure 1. Schematic depiction of the experimental setup for Series 1 (black and red parts of the figure) and Series 2 (black and green parts).

All the added system components were then fed to a second furnace (called the reaction furnace) set to 300/650°C (Series 1) or 650°C (Series 2). Most of the exhaust for that furnace was then sent through a filter followed by a liquid trap, in order to categorize the aerosols and volatile species formed in the reaction furnace, respectively. A portion of the exhaust was

diverted, diluted ten times with N_2 and measured with FTIR (Fourier-Transformed Infrared Spectroscopy), and in the case of Series 1, the TEOM and ELPI systems.
Analysis included ICP-MS (Inductively Coupled Plasma- Mass Spectrometry) of the liquid trap, XPS (X-ray Photoelectron Spectroscopy) and SEM-EDX (Scanning Electron Microscopy- Energy Dispersive X-ray Spectroscopy) of the filters, as well as the data from TEOM and ELPI. The FTIR did not yield any useful results, presumably due to too low concentrations of volatile species at that point of the system.

4. Highlights

The results from the research and the discussion around them can be found in the two papers: "Effects of boric acid on volatile tellurium in severe accident conditions" [7] and "Effect of Boric Acid on Volatile Fission Products in Conditions Simulating a Severe Nuclear Accident" [8]. However, highlights of the papers are briefly discussed here.

4.1. Highlights- "Effects of boric acid on volatile tellurium in severe accident conditions"

This paper [7] investigates interactions between tellurium and boric acid solution without any other fission products present. While no direct interaction (species containing the Te-B chemical bond) could be confirmed, the boric acid had an evident effect. This was most clearly seen with the XPS-analysis where the oxidation level of the analysed filter deposition tended to be lower than the corresponding reference system. A pair of filters (exposed to 650 ^{o}C in 5% H_2 in Ar) were re-measured after spending two weeks in ambient conditions. The reference filter had oxidized significantly, whereas the filter exposed to boric acid solution barely had changed at all, further supporting the theory that boric acid may serve to protect the tellurium metal from oxidation. This potentially has implications for tellurium speciation and behaviour in severe accidents, as tellurium metal is more volatile than tellurium dioxide, and is also chemically different. As such, the presence of boric acid in the severe accident chemistry may affect the tellurium chemical and physical behaviour. Tellurium was transported either as tellurium metal, TeO_2 (in oxidizing conditions) or as H_2Te in reducing atmospheres and high temperature. The transport of boron most likely occurred as B_2O_3, the final product after several dehydration reactions of $B(OH)_3$.
The prevention of oxidation by boric acid is also known in jewellery, where boric acid is used to prevent oxidation ("fire scales") of the metals during soldering.

4.2. Highlights- "Effect of Boric Acid on Volatile Fission Products in Conditions Simulating a Severe Nuclear Accident"

This system included, aside from tellurium and boric acid, also iodine and caesium [8]. The iodine resulted in two effects that are worthy of notice. First, the presence of iodine and tellurium together, mainly in the reducing atmosphere, gave raise to crystals of tellurium iodide, which could be discerned by XPS and confirmed with SEM-EDX where they were clearly visible. Furthermore, there was a drastic change in the tellurium liquid trap concentration when tellurium, iodine vapour and boric acid solution all were present together. In every examined atmosphere, the tellurium concentration increased. The most striking change was in the case of inert atmosphere. The system with boric acid and tellurium (from Series 1) measured 0.78 µM tellurium, the system with iodine and tellurium measured 0.04 µM tellurium, whereas the system using both measured 0.11 mM. There is clearly a synergistic interaction due to the boric acid and the iodine. The exact nature of this interaction is still uncertain, but the hypothesis is that it involves the formation of tellurium iodide in the high temperature regime of the furnace, followed by its decomposition as the temperature

drops. This decomposition would liberate tellurium vapour in a more efficient manner than the normal vaporization and would enable an efficient reaction with the boric acid solution. However, it is not possible to say if the increased volatility is entirely due to boric acid or water. The presence of water does increase tellurium volatility, but it typically requires an oxidizing atmosphere [9], which was not the case for the interaction seen in this study. Furthermore, the XPS analysis never implied the formation of a B-Te bond, making direct interaction with the boric acid unlikely as well. Nevertheless, both iodine and boric acid together in this system resulted in tellurium volatility increasing significantly.
The experiments with CsI did not yield the same result, which is an important consideration since CsI is the most important iodine species released in a nuclear accident. Cs was not detected in the liquid traps but was detected on the filters with the XPS in low quantities. The speciation is either CsI, as could be expected, and/or either CsOH, or some CsTe- species. Due to the low contents and the fact that their signals overlap in the XPS spectrum, it is not possible to differentiate them with certainty.

5. Conclusions

The goal of project TRIO was to investigate the possible impact boric acid may have on tellurium in a scenario similar to a severe nuclear accident. This was done in two experimental series. One of them focused on the interaction between tellurium and boric acid, and the other one expanded the investigation further by also including iodine and caesium iodine. The results for the first experimental series proved that boric acid affects the physical behaviour of tellurium in that its rate of oxidation decreases when boric acid is present in the system. This was determined by XPS analysis. As the melting point of tellurium dioxide is about 730 ^{o}C, compared to 450 ^{o}C of metallic tellurium, this may imply that the presence of boric acid results in potentially more volatilization of tellurium.
When iodine is also included in the system the formation of tellurium iodide is possible, especially in the reducing atmosphere (5% H_2 in Ar). Upon the addition of boric acid to a system containing tellurium and iodine, the tellurium volatility was increased by several orders of magnitude in every atmosphere.
Project TRIO have investigated a hitherto unknown system, focusing on some of the volatile fission products and boric acid. The results imply that there is most likely an indirect effect of boric acid on this system. However, further research on the Te-I-$B(OH)_3$ system is needed to conclusively determine the mechanism responsible for the increase in tellurium volatility when tellurium, iodine and boric acid is present together.

6. Acknowledgements

NKS conveys its gratitude to all organizations and persons who by means of financial support or contributions in kind have made the work presented in this report possible.

7. Disclaimer

8. References

[1] G. Brillant, C. Machetto, W. Plumecocq, 2013, *Fission product release from nuclear fuel I. Physical modelling in the ASTEC code, Annals of Nuclear Energy*, 61, 88–95, http://dx.doi.org/10.1016/j.anucene.2013.03.022, retrieved 2021-11-29

[2] V.Kazakov, E. Demidchik, L. Astakhova, 1992, *Thyroid cancer after Chernobyl*, *Nature*, 359, 21, https://doi.org/10.1038/359021a0, retrieved 2023-05-23.

[3] M. Osaka, M. Gouëllo, K. Nakajima, 2022, *Cesium Chemistry in the LWR severe accident and towards the decommissioning of Fukushima Daiichi Nuclear Power Station*, *Journal of Nuclear Science and Technology*, 59:3, 292-305, DOI: 10.1080/00223131.2021.1997664, retrieved 2022-03-28

[4] J.McFarlane, J.C.LeBlanc*, 1996, Fission product Tellurium and Cesium Telluride Chemistry Revisited*, No. AECL-11333, Atomic Enegry of Canada Ltd., retrieved 2021-10-11

[5] Edward C. Beahm, 1987, *Tellurium Behavior in Containment under Light Water Reactor Accident Conditions*, *Nuclear Technology*, 78:3, 295-302, DOI: 10.13182/NT87-A15995, retrieved 2021-12-01

[6] A-E. Pasi, M. R.St.-J Foreman, C. Ekberg, 2022, *Organic telluride formation from paint solvents under gamma irradiation*, *Nuclear Technology*, 208:11, pages 1734-1744, https://doi.org/10.1080/00295450.2022.2061258

[7] F. Börjesson Sandén, A-E. Pasi, T. Kärkelä, T. Kajolinna, C. Ekberg, 2024, *Effects of boric acid on volatile tellurium in severe accident conditions*, *Annals of Nuclear Technology*, 200, https://doi.org/10.1016/j.anucene.2024.110412

[8] F. Börjesson Sandén, A-E. Pasi, T. Kärkelä, T. Kajolinna, C. Ekberg, 2024, *Effect of Boric Acid on Volatile Fission Products in Conditions Simulating a Severe Nuclear Accident*, *Nuclear Technology*,

[9] A.P. Malinauskas, J.W. Gooch Jr, J.D. Redman, *The Interaction of Tellurium Dioxide and Water Vapor*, *Nuclear Applications and Technology*, vol. 8, 1, pages 52-57, 1969, retrieved 2024-04-04, https://doi.org/10.13182/NT70-A28633

---

9. Appendices

Appendix 1: Effects of boric acid on volatile tellurium in severe accident conditions

Appendix 2: Effect of Boric Acid on Volatile Fission Products in Conditions Simulating a Severe Nuclear Accident

Bibliographic Data Sheet **NKS-500**

Title	NKS- Project TRIO; Tellurium, Iodine and Caesium Interactions with Boric Acid during a Nuclear Accident (2023-2024)
Author(s)	Fredrik Börjesson Sandén[1] Anna-Elina Pasi[2] Teemu Kärkelä[2] Tuula Kajolinna[2] Christian Ekberg[1]
Affiliation(s)	[1]Chalmers University of Technology, Kemivägen 4, SE-412 96 Gothenburg, Sweden [2]VTT Technical Research Centre of Finland Ltd, P.O. Box 1000, FI-02044 VTT, Espoo, Finland
ISBN	978-87-7893-598-4
Date	April 2025
Project	NKS-R / TRIO-activity (Contract: AFT/NKS-R(23)139/6)
No. of pages	8
No. of tables	2
No. of illustrations	1
No. of references	6
Abstract max. 2000 characters	Project TRIO was a project partially funded by NKS 2023-2024, and a joint collaboration between Chalmers University of Technology and VTT technical research institute in Finland. The project aim was to investigate if and how boric acid influences volatile fission product behaviour in severe nuclear accident-like conditions, with a special focus on tellurium. The project was split into two parts, with the first one investigating the influence of just tellurium and boric acid, and the other one also including vaporized Iodine, as well as caesium iodide. The experiments involved volatilization of tellurium into a carrier gas, into which boric acid solution was added. This yielded filters and liquid traps which were analysed, chiefly with ICP-MS and XPS and SEM-EDX. Online aerosol measurements (TEOM and ELPI) were also used. The results imply that there is little direct interaction between tellurium and boric acid, as the Te-B chemical bond is never detected. However, boric acid decreases the tendency for tellurium

to oxidize, and it is part of an interaction involving tellurium, iodine and boric acid all together which results in an increase in tellurium volatility by several orders of magnitude.

Key words Severe Nuclear Accidents, Tellurium, Iodine, Fission Products, Boric Acid

Annals of Nuclear Energy 200 (2024) 110412

Contents lists available at ScienceDirect

Annals of Nuclear Energy

journal homepage: www.elsevier.com/locate/anucene

Effects of boric acid on volatile tellurium in severe accident conditions

Fredrik Börjesson Sandén [a,*], Anna-Elina Pasi [b], Teemu Kärkelä [b], Tuula Kajolinna [b], Christian Ekberg [a]

[a] Chalmers University of Technology, Kemivägen 4, SE-412 96 Gothenburg, Sweden
[b] VTT Technical Research Centre of Finland Ltd, P.O. Box 1000, FI-02044 VTT, Espoo, Finland

ARTICLE INFO

Keywords:
Tellurium
Severe accidents
Boric acid
Fission product
XPS

ABSTRACT

Boric acid is used in light-water nuclear reactors to control the reactor and is expected to be present as part of the chemistry of a severe accident. Therefore, its influence on other prominent species expected in an accident must be investigated. One such species is tellurium. In the present study, tellurium is volatized, and boric acid is dissolved and injected into the system as a means of studying the interaction between it and tellurium. The experiments were evaluated with ICP-MS and XPS. Results suggest that while there is no direct interaction, boric acid still affects the tendency for tellurium to oxidize. In general, less oxidation was detected in the presence of boric acid than in its absence, especially at high temperatures. The species formed upon oxidation was determined to be TeO_2. Since tellurium metal is more volatile than TeO_2, this may have implication in a wider severe accident context.

1. Introduction

Nuclear energy, while being plannable and having negligible emissions of greenhouse gases (Sims et al., 2003), has proven to have certain disadvantages as well. Among the most visible disadvantages is the risk of severe accidents, such as Fukushima and Chernobyl. As such, for nuclear power to be a realistic choice for energy production, such accidents need to be studied and researched carefully to mitigate the consequences. Severe nuclear accidents differ from almost all other industrial accidents because of the presence of radioactive substances. Radiation carries the risk of acute radiation damage if the doses are high enough, but can also trigger carcinogenic diseases much later in life (Kazakov et al., 1992).

The radioactivity present in a nuclear power plant originates from the fuel and activation of structural materials. In the fuel, the radiation level is increased with fuel burnup due to the formation of highly radioactive fission products, such as iodine and cesium, both of which have been studied extensively both in larger experimental programs (March and Simondi-Teisseire, 2013; Clément and Zeyen, 2013) and smaller reports focusing on certain specific phenomena (Hou et al., 2013; Awual et al., 2014). Another notorious fission product is tellurium, which decays to form iodine. The decay means that the tellurium release will function as a delayed source of iodine with the potential to bypass countermeasures specifically targeted to iodine. Chemically, tellurium is highly variable and can occur in several different forms, including as organic species. Compared to iodine and cesium, it is significantly less studied.

A common choice for a neutron absorber in a nuclear reactor is boron, and control rods tend to incorporate this element. They were in use for instance in the Chernobyl plant and the Fukushima-Daiichi plant (boron carbide (Atomic Energy Society of Japan, 2014)). However, the most common reactor type, the pressurized water reactor (PWR), also makes use of dissolved orthoboric acid (henceforth referred to as just "boric acid"), both for regular operation and as an emergency system (Neeb, 1997). This means that boric acid or products derived from it most likely will be present in several chemical forms during an accident scenario. Tellurium and boron are known to interact with each other in certain situations. The oxides TeO_2 and B_2O_3, both of which can potentially form in a nuclear accident, are for instance known to form glasses (Bürger et al., 1984), though the temperature of this reaction exceeds the expected temperatures in the nuclear containment. Nevertheless, formation of similar species would be expected to strongly affect the tellurium behavior, especially the volatility. The aim of this paper is to determine whether tellurium and boron interact in nuclear accident-like conditions and investigate if and how the volatility of tellurium changes due to the presence of boric acid.

* Corresponding author.
E-mail address: sandenf@chalmers.se (F. Börjesson Sandén).

https://doi.org/10.1016/j.anucene.2024.110412
Received 14 December 2023; Received in revised form 26 January 2024; Accepted 5 February 2024
Available online 10 February 2024

2. Theory and background

2.1. Tellurium

Nuclear accidents present complex and variable chemical environments depending on, for example, the reactor type and the accident nature. Temperatures can vary from thousands of degrees inside the reactor core to near ambient temperatures outside of the containment, and atmospheric condition can likewise be oxidizing or reducing due to the reaction between zircalloy and water, with varying levels of steam present.

In total, dozens of tellurium nuclides are known to exist. However, significantly fewer makes for a realistic hazard in an accident scenario, namely those with a long enough half-life to pose a risk to the public after release. For radiation protection purposes, the most relevant tellurium nuclides are ^{129m}Te with a half-life of 33.6 days and ^{132}Te with a half-life of 3.17 days (Magill et al., 2015). Their respective releases during the Fukushima accident was 15 PBq and 180 PBq (Steinhauser et al., 2014).

Tellurium is a chemically complex element which melts at 449.5 °C and boils at 988 °C. It exists in five principal oxidation states (−2, 0, +2, +4 and +6). It belongs to the chalcogen group, same as oxygen. When heated in the presence of oxygen, tellurium forms tellurium dioxide TeO_2. It has a higher melting and boiling point, at 732 °C and 1245 °C respectively, though its volatility can be increased in the presence of steam, possibly due to the formation of $TeO(OH_2)$ (Medina-Cruz et al., 2020). TeO_2 is an amphoteric compound, behaving as a base in acidic media, and as an acid in alkaline media. Its solubility in water is poor. If oxidized further, for instance with hydrogen peroxide, it forms telluric acid $Te(OH)_6$ (Medina-Cruz et al., 2020).

Just like the lighter chalcogens, tellurium can react with hydrogen and form an analogue of water, named hydrogen telluride, H_2Te. It is a colorless gas with a pungent odor which decomposes quickly in air at temperatures below 627 °C. (Garisto, 1992; Medina-Cruz et al., 2020). The thermodynamics of the formation has been reported by Edward (1987). The formation can be expressed as seen in Reaction 1.

$$\frac{1}{2}Te_2(g) + H_2(g) \rightleftharpoons H_2Te(g) \qquad \text{(Reaction 1)}$$

The corresponding equilibrium constant for this reaction is given by Equation 1, where K is the equilibrium constant, and P indicates the different partial pressures. From this reaction, an increase in the H_2/Te ratio (a high partial pressure of hydrogen) pushes the reaction to the right (Garisto, 1992).

$$K = \frac{P_{H_2Te}}{\sqrt{P_{Te_2}} \times P_{H_2}} \qquad (1)$$

Due to the square-root in the denominator, a change in the tellurium partial pressure has a relatively low bearing on the hydrogen telluride. As the tellurium partial pressure decreases, thermodynamically, a proportionally larger part of the tellurium can be expected to appear as H_2Te (Garisto, 1992), though K itself never changes. However, hydrogen telluride decomposes quickly in moisture to form elemental tellurium.

Tellurium can also corrode steel under certain circumstances. If 316 l stainless steel is submerged in molten tellurium at 551 °C, it will corrode the steel and form a scale of metal tellurides on the form MTe_2, where M can be Fe, Cr or Ni. This is a fast process, as Martinelli et al. dissolved a 10x30x0.5 mm steel sample completely in 10 min (Martinelli et al., 2019). The reaction was a direct interaction and dissolution of the alloying elements iron, chromium, and nickel with tellurium (Pulham and Richards, 1990).

2.2. Boron from a nuclear perspective

Boron is present in nuclear installations due to its excellent neutron absorbing properties. In order to safely operate a nuclear reactor, the neutron economy must be carefully maintained. Control rods are used to increase or decrease the reactivity of the core as is needed, and function by being made from a neutron absorbing material. There are several designs where boron-based materials such as boron carbide or boron nitrate are used.

Aside from the control rods, boron has another application PWR: s. In this design, the water in direct contact with the reactor is isolated, meaning that additions to the water directly can be used to change the moderating properties of the water by addition of boron (Connolly, 1978). Typically, the control rods are used to change the neutron flux in the reactor in the short term, while varying the boric acid concentration is used to compensate for long-term changes in the fuel reactivity (Wiesman, 1977). This means that accidents in PWR systems may well include boric acid, or its derivatives, as part of the accident chemistry. Concentrations of boric acid in the primary circuit depends on the freshness of the fuel in the reactor, where fresh fuel necessitates a higher boron concentration. At first startup, when the entire core is using fresh fuel, the concentration can be as high as 2 g/l boron (of natural isomeric composition), and about 1 g/l at the beginning of a normal fuel cycle down to just a few mg at the end of the cycle (Neeb, 1997). In the case of an emergency, a concentrated solution of 2200 ppm of boron is injected (Neeb, 1997).

Boric acid undergoes sequential dehydration as it is heated. The reactions and relevant temperatures are given in the Reactions 2, 3 and 4 (Kaur et al., 2021).

$$B(OH)_3 \rightleftharpoons HBO_2 + H_2O,\ T\ 142^oC \qquad \text{(Reaction 2)}$$

$$4HBO_2 \rightleftharpoons H_2B_4O_7 + H_2O,\ T\ 167^oC \qquad \text{(Reaction 3)}$$

$$H_2B_4O_7 \rightleftharpoons 2B_2O_3 + H_2O,\ T\ 327^oC \qquad \text{(Reaction 4)}$$

$B(OH)_3$ melts 169 °C (Huo et al., 2019), and B_2O_3 at 500 °C (Hildenbrand et al., 1963).

However, thermodynamic calculations seem to indicate that transport of these compounds mainly occurs as boric acid or the trimer of metaboric acid ($H_3B_3O_6$) in temperatures between 180 °C and 727 °C. (Gouëllo et al., 2021). In a nuclear accident scenario, boric acid has previously been shown to be a factor that should be accounted for. In the case of the volatile fission products cesium and iodine, they often appear together as CsI aerosols. Their reaction will depend on the accident scenario, but in the presence of boric acid they can react to form cesium borates and gaseous iodine, according to the Reactions 5 and 6 (Gouëllo et al., 2021).

$$CsI(c) + B(OH)_3(g) \rightleftharpoons CsBO_2(c) + HI(g) + H_2O \qquad \text{(Reaction 5)}$$

$$2HI(g) \rightleftharpoons I_2(g) + 2H_2(g) \qquad \text{(Reaction 6)}$$

Tellurium is chemically different from both iodine and cesium, and its interaction with boric acid is unknown. The purpose of this paper is to investigate the effect of boric acid upon tellurium aerosols in conditions like those in a severe accident. This will be followed by a second paper to study the interactions in the same system, while also including iodine and cesium.

3. Method

A total of twelve experiments were conducted, and the experimental conditions are described in Table 1. Three atmospheric conditions (oxidizing, inert and reducing) were investigated and two temperatures, 300 °C and 650 °C were chosen, as similar temperatures have been used to simulate the primary circuit during a severe accident before (Clément and Zeyen, 2013). Boric acid undergoes its final dehydration at about 330 °C. Thus, with these two temperatures, the boric acid speciation may be different between the two conditions. Finally, boric acid and

Table 1
Experimental matrix for the study of interactions between tellurium and boric acid.

Experiment designation	Temperature [°C]	Atmosphere	Injection
Ref_Ox_LT	300	Oxidizing (Air)	–
Exp_Ox_LT	300	Oxidizing (Air)	$B(OH)_3$ (aq)
Ref_Ox_HT	650	Oxidizing (Air)	–
Exp_Ox_HT	650	Oxidizing (Air)	$B(OH)_3$ (aq)
Ref_In_LT	300	Inert (N_2)	–
Exp_In_LT	300	Inert (N_2)	$B(OH)_3$ (aq)
Ref_In_HT	650	Inert (N_2)	–
Exp_In_HT	650	Inert (N_2)	$B(OH)_3$ (aq)
Ref_Rd_LT	300	Reducing (H_2/Ar)	–
Exp_Rd_LT	300	Reducing (H_2/Ar)	$B(OH)_3$ (aq)
Ref_Rd_HT	650	Reducing (H_2/Ar)	–
Exp_Rd_HT	650	Reducing (H_2/Ar)	$B(OH)_3$ (aq)

water are injected into the carrier gas for all three atmospheric conditions.

Throughout all of these experiments, only singlets were performed, meaning that uncertainty analysis based on repeated experiments is not possible.

3.1. Experimental setup

The system used is one that has been used before to study the volatility of tellurium (Pasi et al., 2023), housed at VTT, Espoo in Finland. It is described in Fig. 1.

Both the reaction furnaces (tubular flow furnaces, Entech Vecstar, VCTF 4) used tubes made of stainless steel (AiSI 316l) to carry out the experiments. The volatilization furnace was set to 540 °C, and the reaction furnace was set to either 300 °C or 650 °C, depending on the experiment. The volatilization furnace was loaded with a total of 5 g tellurium metal powder (Te, Sigma-Aldrich, purity ≥99.997 %), placed in an alumina "boat" crucible in the middle of the heating section. With the slightly higher volatilization temperature compared to the melting point of tellurium, volatilization was relatively even across the experiments. With the high amount of tellurium, several experiments could be run in sequence without the need for the furnaces to cool down, meaning the conditions between most experiments using the same atmosphere could be kept relatively constant.

The experiments in inert and reducing atmosphere were ran in the following order: first the low-temperature reference experiment, followed by the low-temperature experiment with boric acid, followed by the high-temperature reference experiment, and finally the high-temperature acid experiment. Between each experiment, the filters (MilliPore, MitexTM PTFE, pore size 5 μm) and the liquid trap (0.1 M NaOH) were changed. For the oxidizing conditions it was feared that such a process would oxidize all of the precursor (the oxidation reaction is fast enough at 540 °C to affect the release of the tellurium precursor) towards the latter experiments, and so the four oxidizing conditions were conducted in two stages, with the two low-temperature experiments being run in sequence, where after the precursor was changed. The corresponding high-temperature experiments were run in sequence after. Following the experiment completion and the cooldown of the furnaces, the system was washed, and the precursor was retrieved. The mass of the precursor after the experiment was never below 3 g.

In principle the process of forming hydrogen telluride as described in reaction 1, could happen in the volatilization furnace and decrease the availability of tellurium in the latter experiments ran in the reducing atmosphere. However, as hydrogen telluride is unstable at the volatilization temperature, such an interaction is not expected to have any effect on the results.

The total gas flow through the reaction furnace was 6 l/min, supplied from two places; 3 l/min were fed through the volatilization furnace, and 3 l/min were added through the middle junction, alongside the boric acid for the experiments that used it. The gas flows were regulated through mass-flow control units (Brooks S5851, Brooks® Instrument). The water or the boric acid solution was fed through an atomizer (TSI model 3076). The boric acid concentration was 0.2 M.

Following the reaction furnace, 5 l/min of the gas stream was directed through the filter to collect any aerosol particles, and then proceeded through a liquid trap to catch any gaseous species. The final 1 l/min of the gas flow was diverted prior to the filter sampling. This gas was diluted and quenched with 10 l/min N_2 gas and then fed through the online measurement devices FTIR (fourier-transformed infrared spectroscopy), ELPI (electric low-pressure impactor), TEOM (tapered element oscillating microbalance, Rupprecht Patashnick Co., Inc. series 1400A).

Before the experiments began, the system was continuously flushed with N_2 until the setpoint of both furnaces were reached, and each experimental condition lasted for 30 min. After that time had passed, the gas flow was diverted to an exhaust while the filters and liquid traps were changed. After concluding an experiment series, the precursor was also collected for analysis with powder x-ray diffraction (PXRD).

The filters were weighed with a bench scale (Mettler Toledo XPE204) to the precision of one tenth of a milligram before and after the experiment to determine the weight of the collected material. After the filter's

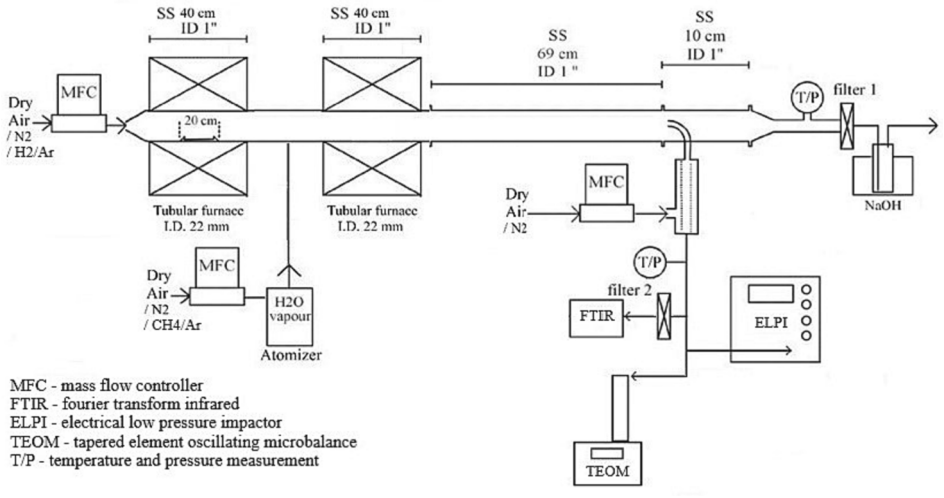

Fig. 1. Schematic depiction of the experimental setup used for the study.

retrieval, it was kept in a petri dish wrapped in parafilm and stored at room temperature. The filters were analyzed with XPS (X-ray photoelectron spectroscopy), within one week.

A mass balance could not be established due to significant deposition of tellurium at the junction between the furnaces, as well as in the tubing after the reaction furnace. Heating bands were used, but proved insufficient to prevent the deposition, especially at the junction where boric acid solution was added.

3.2. Analytical methods

3.2.1. ICP-MS

The elemental content of the liquid traps was measured with High resolution ICP-MS (inductively coupled plasma mass spectroscopy, Element 2, ThermoScientific) to determine the amount and species of the elements capable of penetrating the filters. The detection limit for tellurium (Te^{126}) was 0.006 ppb. The samples were diluted with 0.5 M HNO_3 (Suprapure) for the measurements.

3.2.2. XPS

The XPS machine used to analyze the filters was a PHI5000 VersaProbe III- Scanning XPS Microprobe™, using a monochromatic AlKα x-ray source (1486 eV). The beam width was 100 μm, 25 W 15 kV. FWHM was 0.654 eV. The system was aligned with Au (83.96 eV), Ag (368.21 eV) and Cu (932.62 eV), and the narrow scan measurements were aligned with the C1s signal at 284.6 eV before analysis.

Survey scan proceeded from 0 to 1100 eV with a step size of 1 eV, and the narrow scans proceeded over the selected region for the relevant element, with a step-size of 0.1 eV. For the C1s signal the step size was 0.05 eV.

3.2.3. PXRD

The precursors were analyzed in PXRD. The instrument was Bruker D8 Discover with a Cu Kα x-ray source. Measurement began at 20° and ended at 80°. The current and voltage in the X-ray source was 40 mA and 40 kV, respectively. Analysis was performed with the DIFFRAC.EVA software, version 5.2.

3.3. XPS binding energies and sensitivity factors

XPS (X-ray photoelectron spectroscopy) is a surface sensitive method of analysis that can be used to identify elements and their relative abundance in a sample. Furthermore, the chemical state of the elements in the sample can also be determined by XPS, through shifts in the measured binding energy. Table 2 lists several species relevant for tellurium and boron, and the binding energies associated with them (NIST X-ray Photoelectron Spectroscopy Database, 2012). The tellurium chemical state was investigated based on the $3d_{5/2}$-signal, and the oxygen and boron were both investigated based on their respective 1S signal.

Elemental compositions of the examined surfaces can be calculated according to Eq. (2)

$$C_x = \frac{\frac{I_x}{S_x}}{\sum_i \frac{I_i}{S_i}} \quad (2)$$

Where "I" is the measured peak area, "S" is the designated peak sensitivity factor, subscript "x" is the species of interest, subscript "i" is every species in the sample, and C is the calculated amount of element x in the sample surface (Stevie and Donley, 2020). The sensitivity factors account for the fact that different signals are easier to measure than others, with a high sensitivity factor for a signal indicating it is easily measured. This also means that a very clear signal does not necessarily mean a high concentration of that element in the sample. The calculation of the surface composition is based on the specific signals and sensitivity factors listed in Table 3.

The sensitivity factors used are supplied by the software used for the analysis; MultiPak Version 9.7.0.1, Ulvac-phi inc. Note that the analysis of the chemical state for tellurium is based on the $3d_{5/2}$- signal, and the abundance calculation uses the 4d-signal.

Table 2
Binding energies for various compounds as measured by XPS (NIST X-ray Photoelectron Spectroscopy Database, 2012). There is no reported energy level for the oxygen of TeO_3 or $Te(OH)_6$.

Compound	Binding energy (Te-$3d_{5/2}$) [eV]	Binding energy (B- 1S) [eV]	Binding energy (O-1S) [eV]
Te	572.9–573.54	–	–
TeO_2	575.6 eV- 576.5	–	530.1–530.7
TeO_3	576.6–577.3	–	–
TeO_3*$3H_2O$ (or $Te(OH)_6$)	577.1	–	–
B	–	186.5–188.5	–
$B(OH)_3$	–	192.8–193.6	533.4
B_2O_3	–	192.0–193.7	532.5–533.8

4. Results and discussion.

4.1. Filter weights

The filters were weighted with a bench scale with the precision of one tenth milligram before and after the experiment. The mass accumulated on the filters during the experiments can be seen in Fig. 2.

Two things are clear: there is a decreasing trend as the experiment progresses, and the reducing conditions consistently give the highest mass of aerosol particles on the filters. The decreasing trend can be explained by small leaks in the system, admitting some oxygen even in the case of inert and reducing conditions. This was seen on the precursor after the experiments and affected the inert systems more than the reducing one, presumably as the oxygen reacted to form water in the latter case. This then explains the higher filter mass for the early experiments, as the oxidation of the precursor increased gradually. For the oxidizing conditions a similar logic applies. Since those experiments were performed in two parts with fresh precursor for the high- and low-temperature experiments, the high masses in both the oxidizing reference cases can be justified; since those experiments used fresh precursor, some unoxidized tellurium reaches the filter and contributes to the weight. After some time in the oxidizing conditions, when the experiment with the acid begins, the precursor is largely oxidized already in the crucible and very little material can volatize and reach the filter.

As only singlets are performed, and due to progressive decrease in the filter mass accumulation, it is not possible from this result alone to certainly state that transportation of tellurium aerosols increase due to the addition of boric acid. However, it is worth pointing out that the high-temperature experiment with boric acid added does show a small increase in filter mass for both the inert and reducing conditions, even though the precursor should become less and less accessible as the experiment progresses. It seems like the acid solution may induce a slight increase in tellurium volatility. This idea is reinforced by the XPS measurements, which indicates that oxidation happens to a lower degree in the systems involving the acid solution (see further chapter 4.5.). As oxidation decreases volatility in tellurium, these two results are

Table 3
Signals and their associated sensitivity factors used to calculate the relative compositions of the investigated surfaces.

Element	Signal	Sensitivity factor
Te	4d	1.721
B	1 s	0.171
O	1 s	0.733
C	1 s	0.314

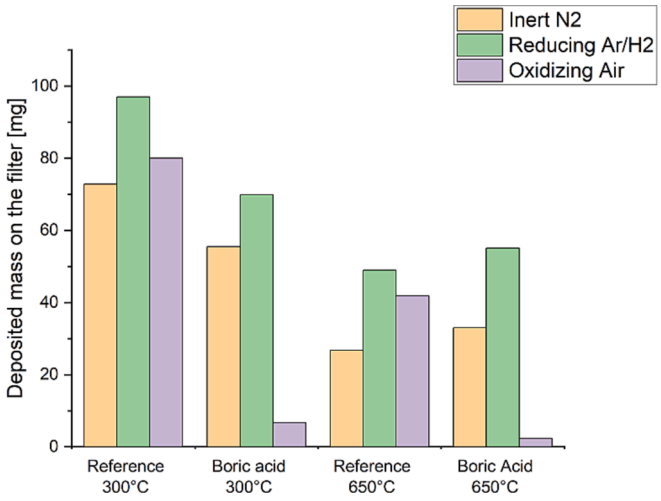

Fig. 2. Total material accumulated on each main-line filter after the respective experiment.

congruent.

4.2. Contents of the liquid traps

The contents of the liquid traps for the experiments can be found in Table 4. In general, the tellurium content of the liquid traps was very low except for in the high-temperature experiments in the reducing conditions. Boric acid, on the other hand, seems more likely to appear as a gaseous species at elevated temperatures, as the boron content is increased at the higher temperature.

ICP-MS does not allow for determination of chemical species, so it cannot be used to prove or disprove the presence of a Te-B species. However, if such a species forms, it should reasonably cause a change in the tellurium concentration compared to the corresponding reference case. In Table 4, this is seen twice, for the reducing and inert systems at high temperature.

For the high temperature experiments in the reducing atmosphere, the increase in tellurium content can possibly be explained by the formation of hydrogen telluride (H_2Te) in the reference case. The temperature of 650 °C is just high enough to enable its formation. If hydrogen telluride is formed in the high temperature reducing reference experiment, then it could also explain the decrease in tellurium content at the experiment involving boric acid. Since the acid was introduced dissolved in water, and hydrogen telluride decomposes in moist atmospheres, the reduction of tellurium content in the liquid trap in this case could be explained.

The high temperature experiment in inert atmosphere also display slightly more tellurium than the reference case, indicating that a Te-B could potentially be formed in this case. However, there is no indication of this when performing the XPS analysis, see further section 4.5. There is also no mention of any such species in the literature in similar conditions.

The contents of boron are slightly skewed by its presence in the glassware used for the liquid trap which explains the boron content in the reference cases. However, all experiments involving boric acid display heightened concentrations of boron, compared to the respective reference case. This applies for both high and low temperatures, though the increase is significantly higher at 650 °C.

Both the inert and the oxidizing atmosphere show comparatively high content of boron, indicating that boron can be transported as a volatile compound, or as a tiny aerosol (see further details in section 4.3-Online Analysis of Particles). At these temperatures, $B(OH)_3$ is expected to dehydrate quickly into B_2O_3, which has a negligible vapor pressure even at temperatures much higher than 650 °C (Cole and Taylor, 1935), implying transport as aerosols. The comparatively low boron content in reducing conditions implies that boron is less volatile in such an atmosphere. This may be tied to the large variance in particle diameter in reducing conditions (see section 4.3, and section 5.) though this assumption is not congruent with what is seen in from the XPS measurements (section 4.5), as no significant increase in boron content on the filter is detected at reducing conditions.

Table 4
Tellurium and boron contents of the liquid traps for the different experiments. Notice the different units for tellurium and boron.

Experiment Designation	Tellurium content [μmol/dm^3 trap solution]	Boron Content [mmol/ dm^3 trap solution]
Ref_In_LT	2.35	0.17
Exp_In_LT	2.35	1.57
Ref_In_HT	0	0.24
Exp_In_HT	0.78	6.15
Ref_Rd_LT	0.78	0.59
Exp_Rd_LT	0.78	0.75
Ref_Rd_HT	41.5	1.11
Exp_Rd_HT	7.05	3.27
Ref_Ox_LT	0.78	0.13
Exp_Ox_LT	0.78	2.16
Ref_Ox_HT	0.78	0.23
Exp_Ox_HT	0.78	10.37

4.3. Online analysis of particles

The properties of aerosols were online analyzed using ELPI and TEOM devices. The above given results for the accumulated mass of particles on filter were supported by the devices. Further details were extracted from the ELPI data to estimate the development of particle size in the experiments, see Fig. 3.

In general, the highest particle count median diameter (CMD) values were for the inert condition, except at high temperature reference condition in which reducing conditions resulted in the largest particle diameter. The CMD values decreased from inert to reducing conditions and from reducing to oxidizing conditions. It was expected the particle diameter to be low due to the low release of tellurium in an air

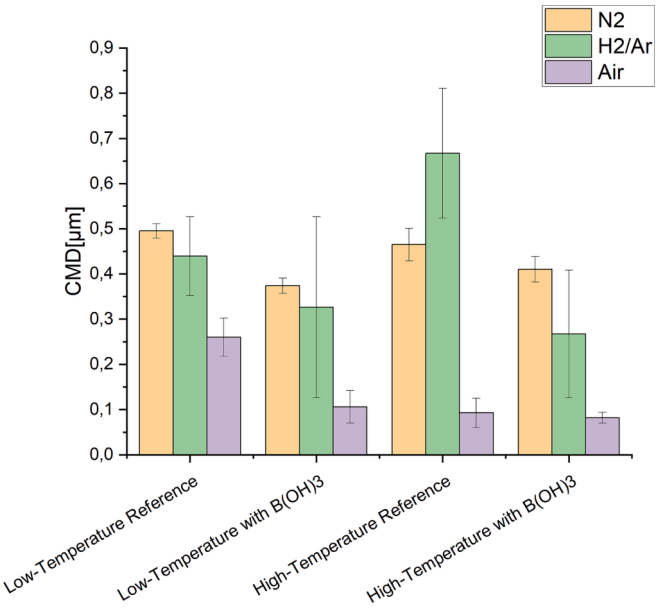

Fig. 3. Particle count median diameter (CMD) in the experiments. The average CMD with the actual minimum and maximum CMD values are given.

atmosphere (tellurium oxidation in the crucible decreases the release). The span of particle diameters was relatively low for both oxidizing and inert conditions, but much bigger for the reducing case.

4.4. FTIR analysis of gaseous species

The properties of gas phase species were online analyzed using FTIR device. In general, the analysis results were showing the expected fed component H_2O with some trace level CO_2 and CO from the laboratory air. The water content ranged ca. from 0.9 to 1.3 vol-% in the experiments and water was observed when boric acid solution was fed using atomizer.

4.5. XPS analysis of the filters

The results for the XPS consists of, for each sample, a survey scan to determine the elemental composition and abundance, as well as a more detailed scan over a small energy range in order to determine the chemical environment of each element. The following section will only present a selection of representative or important spectra. In most cases the survey spectrum looks nearly identical between the samples, differing only in the relative intensities between the peaks. An example of such a spectrum is seen in Fig. 4.

The XPS spectrum for the reference cases in inert and reducing conditions look similar for both the high and low temperature experiments. The spectra for the low-temperature experiment for the inert and the reducing conditions are presented in Fig. 5.

All systems exhibit the same tellurium speciation; one signal is in the area 573.01 eV- 573.12 eV, and another at 576.32 eV- 576.48 eV. Furthermore, the distribution of metallic tellurium and Te(IV) between the systems, and the element composition of the systems both remain almost constant, as can be seen in Table 5. The lower energy signal matches the reported measurements for pure tellurium metal reasonably well. The second signal matches the values reported for TeO_2. Both of these compounds are also reasonable considering the systems; metallic tellurium is the dominant species, with some contamination from oxygen, forming TeO_2.

The appearance of Te(IV) in both the reducing and inert conditions is considered the "baseline" content of Te(IV) for the filters. Most likely this comes from trace amounts of oxygen left in the system during the experiments, or from the time the filters are exposed to the open air in between the experiment and the XPS measurement. The filters retrieved from the inert atmosphere were measured in the XPS only after 7 days, whereas the experiments conducted in reducing atmosphere were measured after 4 days. As can be seen in Table 5, the samples from the reducing atmosphere had a slightly higher ratio of Tellurium metal to Tellurium oxide. However, the relative amount of TeO_2 and tellurium metal were rather similar across all reference cases.

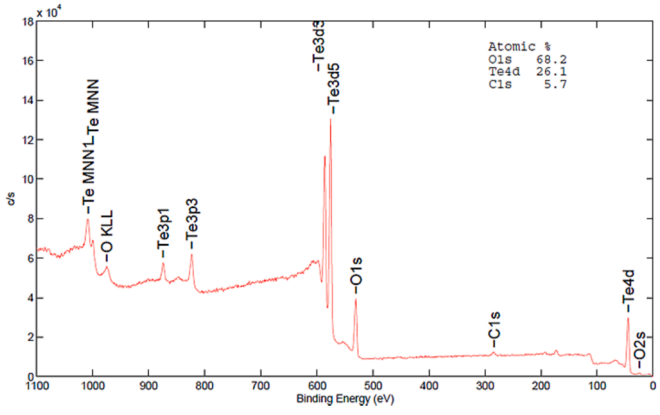

Fig. 4. Survey spectrum of the High-temperature reference spectrum in air atmosphere. The sample predictably contains tellurium, oxygen, and a small contamination of carbon, most likely dust from the sample transport.

The oxygen content is comparatively high relative to the ratio of metallic to oxidized tellurium. However, considering the system with only tellurium and a reducing or inert carrier gas, and the binding energies of the XPS measurements, no other species than TeO_2 can reliably explain the Te(IV) oxidation state. The high-temperature references especially give slightly conflicting results in that the survey measurement imply a large oxidation, whereas the detailed scan of the 3d 5/2 signal instead indicates mostly metallic tellurium.

The oxidizing system behaved differently. The spectrum for both the high- and the low-temperature conditions are displayed in Fig. 6.

As could be expected, the amount of unoxidized metal is very low or completely absent in this system. The + IV oxidation state dominates the high-temperature system completely, whereas the low-temperature system consists of roughly equal parts of a compound with the binding energy 576.17 eV, presumably TeO_2, and a compound with the binding energy 578.03 eV. This energy is higher than any tellurium-oxygen species listed in the database. It is presumed to indicate TeO_3. Since the trioxide is less stable than the dioxide, this assumption explains why the + VI state is not seen in the high-temperature reference.

4.5.1. XPS results- added boric acid solution

The survey spectra again look almost the same for all cases, both high and low temperature experiment, with the one difference being the boron content of the filters. The measured boron contents for the respective samples can be found in Table 6. A comparison of two surveying spectra can be seen in Fig. 7.

For the three low-temperature experiments conducted in the presence of boric acid solution, the XPS measurement of the inert and reducing systems all look very similar to their respective reference cases, as seen in Fig. 8. There is nothing in any of the tellurium spectra that indicates a new species, though there are signals for boron, as well as a change in the oxygen spectrum, matching the oxygen signal for boric acid or B_2O_3 (NIST X-ray Photoelectron Spectroscopy Database, 2012).

While no new tellurium species form, the ratio of metallic to oxidized tellurium has changed due to the addition of boric acid solution, as can be seen in Table 6. While not a large change, the ratio has shifted towards less oxidation compared to the reference cases.

For the high temperature experiments, there is again no indication that tellurium has interacted directly with the boric acid, or any products formed from it. Again, the tellurium spectra are similar to their reference cases for their respective atmosphere.

Furthermore, the degree of oxidation on the sample has changed significantly compared to the reference cases. The oxidizing condition results in complete oxidization of the tellurium to TeO_2, which is not unexpected. However, the low amount of oxidation on the samples from the reducing and inert conditions compared to the references seems to indicate that the oxidation process is inhibited to some degree. See also Table 6. Both in high- and low- temperature conditions all the cases where acid solution is included display significantly lower amounts of Te (IV), indicating that the presence of boric acid serves to further reduce the metal or, more likely, preventing its oxidation.

This may have to do with the pattern seen in Table 4. The increase in tellurium content in the liquid traps following the boric acid experiments may be due to decreased oxidation in those cases. The high temperature reducing condition is the only system where this increase was not seen, but in this case the tellurium can already form a volatile compound in H_2Te.

The oxidizing cases both for high-and low temperature conditions display significant contents of boron, something which is not seen for reducing or inert conditions. Studying the respective high-resolution spectrum places the boron binding energy at 192.9–193.5 eV for every case but one. The low-temperature experiment with boric acid in air has the boron signal also at 195.4. This spectrum is shown in Fig. 9 the 193-signal is assumed to belong to boric acid or B_2O_3. These are difficult to

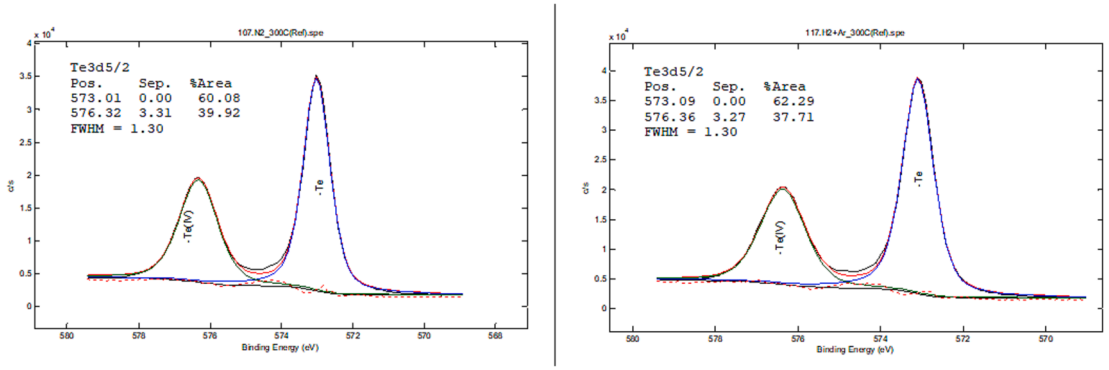

Fig. 5. The XPS spectra of the reference cases. The spectra on the left-hand side are for the inert system, and the right-hand side are for the reducing system, both at the temperature of 300 °C.

Table 5
Contents of the reference filters, and the ratio between Tellurium metal and TeO_2 in the references for reducing and inert atmosphere. Note that the contents do not add up to 100 %. This is due to some interference from the underlying PTFE-filter.

System	Te- content [%]	O- content [%]	Te/Te(IV) ratio in the $3d_{5/2}$ signal
Ref_In_LT	47.2	52.8	1.8
Ref_Rd_LT	54.8	45.2	1.9
Ref_Ox_LT	30.6	69.4	0.1
Ref_In_HT	37.2	62.8	1.6
Ref_Rd_HT	50.5	49.5	1.9
Ref_Ox_HT	27.7	72.3	0

differentiate in the XPS, as both the boron and the oxygen signals tend to overlap. As for the signal at 195.4 eV, it fits reasonably well with boron fluorides BF_4^-, which could, in theory be formed from the fluoride in the PTFE-filter.

4.5.2. Results of remeasurement

To further investigate the hypothesis that the boric acid protects against oxidation, the high-temperature samples from the reducing atmosphere (both the reference sample and the sample exposed to boric acid) were measured again with the XPS. This measurement took place 13 days after the initial measurement, and the samples were exposed to the air in the meantime. The surface composition of the measured filters is reported in Table 7.

It appears that the presence of the boron compound, whether it is boric acid or B_2O_3, does indeed prevent oxidation of tellurium in ambient conditions. Of course, the above result has only been confirmed for the filters treated in reducing conditions. This result may be linked to a study performed by Zhang et al., where 316l steel was submerged in boric acid solutions for seven days. The EDX imaging of those surfaces revealed comparatively little oxygen content, compared to non-borated solutions (Zhang et al., 2018).

5. Conclusions

The presence of boric acid does not seem to result in any compounds composed of tellurium and boron together at the studied low temperature conditions of 300 and 650 °C. However, the presence of boric acid does seem to influence the tellurium in that the oxidation behavior changes upon exposure to boric acid. The XPS measurements consistently showed less oxidation on the samples exposed to boric acid than the corresponding reference samples. For the high-temperature experiments, this is supported by the filter wights, as they increase for the high temperature cases with boric acid compared to without. The theory thus is that boric acid or, perhaps more likely, B_2O_3 is deposited on the

Table 6
Ratio between Tellurium metal and TeO_2 in the experiments including boric acid.

System	Te- content [%]	O- content [%]	B-content [%]	Te/Te(IV) ratio
Exp_In_LT	52.5	39.8	8.5	2.4
Exp_Rd_LT	47.2	46.0	6.8	2.2
Exp_Ox_LT	9.1	67.1	21.7	0.1
Exp_In_HT	54.5	41.8	3.7	3.5
Exp_Rd_HT	54.2	34.4	11.3	3.0
Exp_Ox_HT	5.2	69	25.8	0

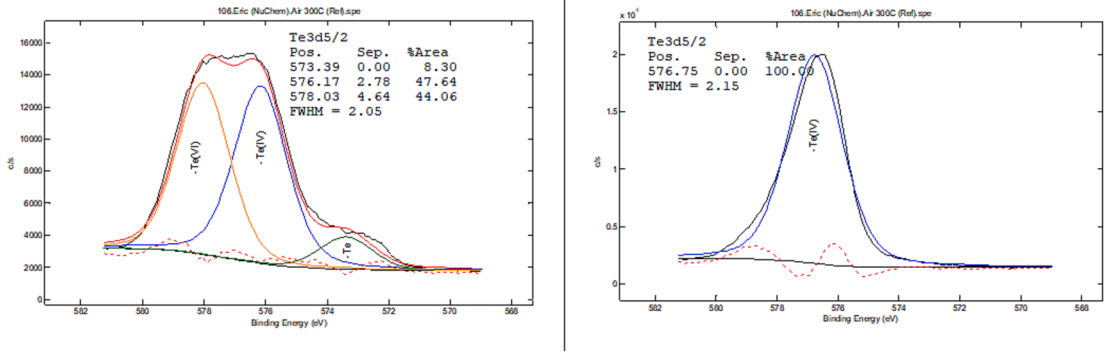

Fig. 6. The XPS spectra of the oxidizing reference cases. The spectrum on the left-hand side is for the system at 300 °C, and the right-hand side is for the system at 650 °C.

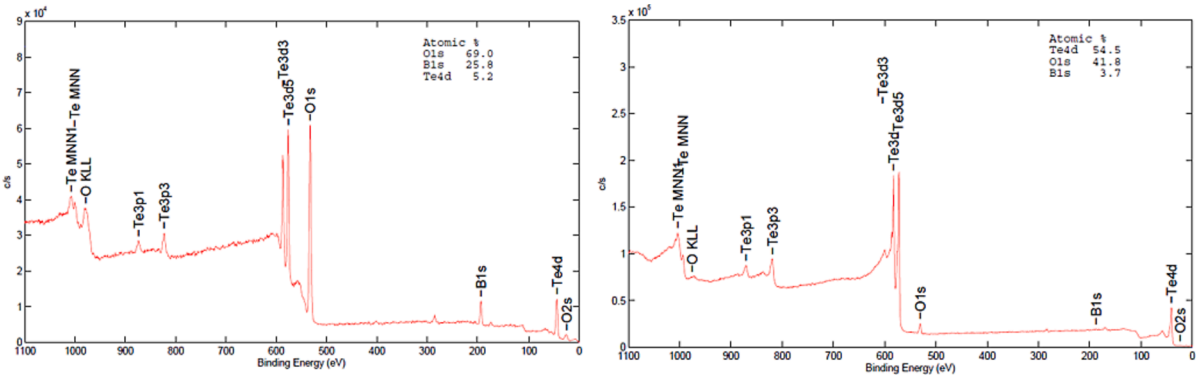

Fig. 7. Survey spectra of the experiments in high temperature involving boric acid. To the left, the experiment conducted in air, and to the right the experiment conducted under nitrogen atmosphere. Notice the different relative signal strength in the boron, at ca. 200 eV.

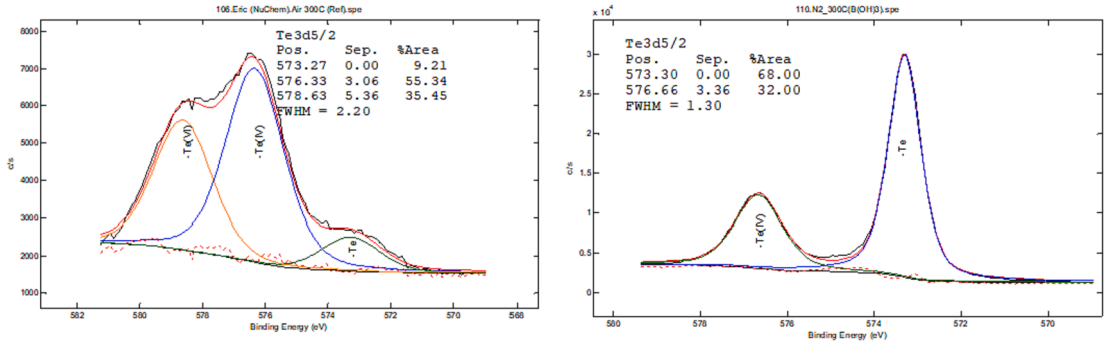

Fig. 8. XPS spectra for the experiments involving boric acid at 300 °C. To the right is the spectrum for inert conditions, which is nearly identical to the spectrum for reducing conditions. On the left is the spectrum for oxidizing conditions.

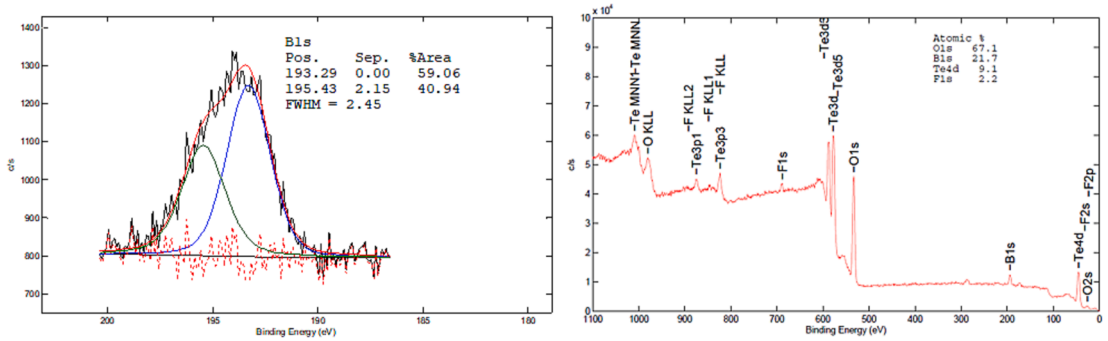

Fig. 9. High-resolution boron spectrum from the low temperature experiment in air atmosphere to the left. The signal is made up of two compounds, where one is either $B(OH)_3$ or B_2O_3. To the right is the corresponding survey spectrum, with the fluoride signal marked (around 700 eV).

Table 7
Change in filter surface composition for the filters exposed to high temperature and reducing conditions after 13 days of exposure to ambient conditions. The filter exposed to boric acid was almost unchanged.

Experiment	Initial measurement			Repeat measurement (Thirteen days later)		
	Te [%]	O [%]	B[%]	Te [%]	O [%]	B[%]
Ref_Rd_HT	50.5	49.5	–	29.1	70.9	–
Exp_Rd_HT	54.2	34.4	11.3	54.0	33.0	13.0

surface on the tellurium particles or alternatively on the filter and form a protective coating that prevents oxidation.

Tellurium is likely transported mainly as TeO_2 in oxidizing conditions, TeH_2 and tellurium aerosols in reducing conditions, and aerosols in inert conditions.

The transport of boron is less certain, as there is contamination from borosilicate glassware in the liquid trap, but there is indication that the transport of boron depends on the atmosphere and temperature. In the liquid trap, the boron content invariably increases for the high-temperature conditions, implying the formation of a compound capable of penetrating the filter. This increase is the largest in oxidizing conditions, though the effect is clearly seen in every condition.

The species responsible for the increase is presumed to be B_2O_3 as an aerosol. The dehydration reaction described in Reactions 2–4 are expected to be faster in the higher temperature, explaining the boron increase in the liquid trap in these cases. As for the increase in the oxidative atmosphere, it is assumed that a direct reaction between oxygen and boric acid complements the dehydration reaction. The overall reaction is presented in Reaction 7.

$$4\,B(OH)_3(g) + O_2(g) \leftrightharpoons 2B_2O_3(s) + 3\,H_2O\,(g) \qquad \text{(Reaction 7)}$$

The XPS-analysis of the filters also detects boron. For both inert and reducing conditions the contents are low, but the oxidizing conditions have significant amounts of boron in both temperatures. This then implies that boron may be transported as an aerosol in oxidizing conditions, though there is no indication in XPS of it being a Te-B-species. Again, it is presumed to be in the form of B_2O_3.

Under the investigated conditions, boron tends to appear in relatively high concentration in both in the liquid trap and on the filter in oxidizing conditions, or in modest amounts in both the trap and on the filter for reducing conditions. This implies that transport of boron happens as a tiny aerosol, somewhat capable of penetrating the filter. The ELPI measurements may also support this theory, as the oxidizing conditions measured the lowest mean particle diameter of all the conditions, implying smaller particles in this case.

CRediT authorship contribution statement

Fredrik Börjesson Sandén: . **Anna-Elina Pasi:** Writing – review & editing, Visualization, Software, Methodology, Formal analysis, Data curation, Conceptualization. **Teemu Kärkelä:** Writing – review & editing, Visualization, Supervision, Methodology, Investigation, Formal analysis, Data curation. **Tuula Kajolinna:** Formal analysis. **Christian Ekberg:** Writing – review & editing, Supervision, Funding acquisition.

Declaration of competing interest

The authors declare that they have no known competing financial interests or personal relationships that could have appeared to influence the work reported in this paper.

Data availability

Data will be made available on request.

Acknowledgements

This work was funded in part by the Nordic nuclear safety research organization (NKS) and APRI 11 (Accident Phenomena of Risk Importance, swedish nuclear safety research). Part of this work was performed at the Chalmers Material Analysis Laboratory, CMAL.

A special thanks to Eric Tam for assistance with the XPS analysis.

References

Atomic Energy Society of Japan, The Fukushima Daiichi Nuclear Accident-Final Report of the AESJ Investigation Committee, Maruzen Publishing Co., 2014, 508-514, 10.1007/978-4-431-55160-7, ISBN 978-4-431-55160-7, retrieved 2023-05-23.

Awual, M.R., Suzuki, S., Taguchi, T., Shiwaku, H., Okamoto, Y., Yaita, T., 2014. Radioactive cesium removal from nuclear wastewater by novel inorganic and conjugate absorbents. Chem. Eng. J. 242, 127–135. https://doi.org/10.1016/j.net.2021.10.026, retrieved 2023-09-13.

Beahm, E.C., 1987. Tellurium behavior in containment under light water reactor accident conditions. Nucl. Technol. 78 (3), 295–302. https://doi.org/10.13182/NT87-A15995, retrieved 2021-12-01.

Bürger, H., Vogel, W., Kozhukharov, V., Marinov, M., 1984. Phase equilibrium, glass-forming, properties and structure of glasses in the TeO_2-B_2O_3 system. J. Mater. Sci. 19, 403–412. https://doi.org/10.1007/BF00553563, retrieved 2023-05-16.

Clément, B., Zeyen, R., 2013. The objectives of the Phébus FP experimental programme and main findings. Ann. Nucl. Energy 61, 11–22. https://doi.org/10.1016/j.anucene.2013.03.037, retrieved 2021-11-29.

Cole, S.S., Taylor, N.W., 1935. The System Na2O-B2O3 IV Vapor pressures of boric oxide, sodium metaborate and and sodium diborate between 1150°C and 1400°C. J. Am. Ceram. Soc. 18, 82–85 retrieved 2023–12-01.

Connolly, T.J., 1978. Foundations of Nuclear Engineering. John Wiely & Sons Inc., pp. 207–282 retrieved 2023–09-13.

Garisto, F., 1992. Theromydnamic behaviour of Tellurium at high temperatures. INIS report nr: AECL—10691, retrieved 2023–05-30, Canada.

Gouëllo, M., Hokkinen, J., Suzuki, E., Horiguchi, N., Barrachin, M., Cousin, F., 2021. Interaction between caesium iodide particles and gaseous boric acid in a flowing system through a thermal gradient tube (1030 K–450 K) and analysis with ASTEC/SOPHAEROS. Prog. Nucl. Energy 138. https://doi.org/10.1016/j.pnucene.2021.103818, retrieved 2022-08-19.

Hildenbrand, D.L., Hall, W.F., Potter, N.D., 1963. Thermodynamics of vaporization of lithium oxide, boric oxide, and lithium metaborate. J. Chem. Phys. 39 (2), 296–301. https://doi.org/10.1063/1.1734245, retrieved 2023-11-03.

Hou, X., Povinec, P.P., Zhang, L., Shi, K., Biddulph, D., Chang, C., Fan, Y., Golser, R., Hou, Y., Ješkovský, M., Jull, A.J.T., Liu, Q., Luo, M., Steier, P., Zhou, W., 2013. Iodine-129 in seawater offshore Fukushima: distribution, inorganic speciation, sources, and budget. *Environ. Sci. Technol.* 47, 3091–3098. https://doi.org/10.1021/es304460k, retrieved 2023-09-13.

Huo, I., Zhu, Q., Li, S., Gao, J., Wang, Q., 2019. Effective assembly of a novel aluminum-oxynitride BaAl11O16N activated by Eu2+ and Mn2+ via salt-flux assistance and its photophysical investigation. J. Alloy. Compd. 787, 96–103. https://doi.org/10.1016/j.jallcom.2019.02.038, retrieved 2023-11-03.

Kaur, G., Kainth, S., Kumar, R., Sharma, P., Pandey, O.P., 2021. Reaction kinetics during non-isothermal solid-state synthesis of boron trioxide via boric acid dehydration. Reaction Kinet., Mech. Catal. 134, 347–359. https://doi.org/10.1007/s11144-021-02084-8, retrieved 2023-04-27.

Kazakov, V., Demidchik, E., Astakhova, L., 1992. Thyroid cancer after chernobyl. Nature 359, 21. https://doi.org/10.1038/359021a0, retrieved 2023-05-23.

Magill, J., Pfennig, G., Dreher, R., Sóti, Z., Nuklidkarte-, K., 2015. Chart of the Nuclides, 9th ed. Nucleonica GmbH. ISBN 978-3-943868-04-3.

March, P., Simondi-Teisseire, B., 2013. Overview of the facility and experiments performed in Phébus FP. Ann. Nucl. Energy 61, 11–22. https://doi.org/10.1016/j.anucene.2013.03.040, retrieved 2021-11-29.

Martinelli, L., Young, D.J., Gossé, S., Bosonnet, S., 2019. Corrosion of 316L in liquid tellurium at 551 °C. Corros. Sci. 151, 35–43. https://doi.org/10.1016/j.corsci.2019.02.001, retrieved 2023-05-31.

D. Medina-Cruz, W. Tien-Street, A. Vernet-Crua, B. Zhang, X. Huang, A. Murali, J. Chen, Y. Liu, J. Miguel Garcia-Martin, J. L. Cholula-Díaz, T. Webster, edited by : B. Li, T. Fintan Moriarty, T. Webster, M. Xing, Racing towards the Surface- Antimicrobial and Interface Tissue Engineering, Springer Nature Switzerland, 2020, ISBN 978-3-030-34470-2, https://doi.org/10.1007/978-3-030-34471-9, retrieved 2023-05-16.

Neeb, K.H., 1997. The Radiochemistry of Nuclear Power Plants With Light Water Reactors, Walter de Gruyter, 1997, pages 27-42, 477-495 retrieved 2021-08-11.

NIST X-ray Photoelectron Spectroscopy Database, NIST Standard Reference Database 20, version 4.1, last update to data content 2012, compiled by A.V. Naumkin, A. Kraut-Vass, S.W. Gaarenstroom, C.J. Powell, DOI:https://doi.org/10.18434/T4T88K, retrieved 2023-06-26.

Pasi, A.E., Kärkelä, T., Börjesson Sandén, F., Tapper, U., Kajolinna, T., Ekberg, C., 2023. Gas phase interactions between tellurium and organic material in severar nuclear accident scenarios. Ann. Nucl. Energy retrieved [2023-11-13].

Pulham, R.J., Richards, M.W., 1990. Chemical reactions of cesium, tellurium and oxygen with fast breeder reactor cladding alloys- part 1, the corrosion by tellurium. J. Nucl. Mater. 171, 319–326. https://doi.org/10.1016/0022-3115(90)90378-Z, retrieved 2023-09-12.

Sims, R.E.H., Rogner, H.H., Gregory, K., 2003. Carbon emission and mitigation cost comparison between fossil fuel and renewable energy resources for electricity generation. Energy Policy 31, 1315–1326. https://doi.org/10.1016/S0301-4215(02)00192-1, retrieved 17/5-2023.

Steinhauser, G., Brandl, A., Johnson, T.E., 2014. Comparison of the Chernobyl and Fukushima nuclear accidents: A review of the environmental impacts. Sci. Total Environ. 470–471, 800–817. https://doi.org/10.1016/j.scitotenv.2013.10.029 retrieved 2021-11-25.

Stevie, F.A., Donley, C.L., 2020. Introduction to X-ray photoelectron spectroscopy. J. Vac. Sci. Technol. A 38, 6. https://doi.org/10.1116/6.0000412, retrieved 2023-011-08.

Wiesman, J., 1977. Elements of Nuclear Reactor Design, Elsevier Scientific Publishing Company, Printed in Amsterdam, pages 1-47, retrieved 2023-09-13.

Zhang, S., Lu, Q., Xu, Y., He, K., Liang, K., Tan, Y., 2018. Corrosion behaviour of 316L stainless steel in boric acid solutions. retrieved 2023-11-30 Int. J. Electrochem. Sci. 13 (4), 3246–3256. https://doi.org/10.20964/2018.04.33,.

Effect of Boric Acid on Volatile Fission Products in Conditions Simulating a Severe Nuclear Accident

Fredrik Börjesson Sandén[1*], Anna-Elina Pasi[2], Teemu Kärkelä[2], Tuula Kajolinna[2], Christian Ekberg[1]

[1]Chalmers University of Technology, Kemivägen 4, SE-412 96 Gothenburg, Sweden

[2]VTT Technical Research Centre of Finland Ltd, P.O. Box 1000, FI-02044 VTT, Espoo, Finland

Corresponding author: sandenf@chalmers.se

Boric acid is expected to play a role in severe nuclear accident chemistry, raising questions of how it affects the volatile fission products iodine, cesium, and tellurium. Experiments were undertaken at VTT Technical Research Center of Finland, using a setup involving the volatilization of tellurium and the injection of iodine as a gas, and boric acid and/or CsI dissolved in water and injected with the help of an atomizer. Analysis of the results included ICP-MS, SEM and XPS.

Results indicate formation of tellurium iodide is possible. It also appears that tellurium may occur as a gaseous species under certain conditions, specifically when volatized with boric acid and iodine together. These results imply that studies of tellurium in combination with other relevant species should be continued. There is evidence that their volatility can be affected by one another, but the research into this type of interaction is scant.

Keywords: Volatile Fission Products, Tellurium, Iodine, Boric Acid, XPS.

1. Introduction

Nuclear accidents differ from most other industrial accidents in that can result in radioactive releases. Even if acute radiation sickness can be avoided, there is a risk of carcinogenesis later in life due to radiation exposure. The fission product iodine is especially notorious, as it is accumulated in the thyroid gland, and radioactive iodine thus is concentrated and the exposure is prolonged, potentially leading to cancer related diseases long after the accident and the exposure [1].

Furthermore, other radioactive isotopes, for instance ^{137}Cs, make radioactive contamination an issue that can last for decades, due to its long half-life. Especially volatile fission products can feasibly escape the reactor containment after an accident and be released to the environment. The volatile fission products are the noble gases iodine, cesium and tellurium[2].

Fission products can react with and form compounds with one another or surrounding elements. These compounds present different chemical, physical and biological characteristics, all of which affect the spread and exposure of radioactivity. Investigations into the chemistry of volatile fission products is a way to predict and mitigate the damage they can do to humans and to the environment in case of a severe nuclear accident.

The most widely used nuclear reactor is the pressurized water reactor (PWR). To control its reactivity, and as part of the emergency shutdown sequence, boric acid is often dissolved in the primary circuit. Natural boron contains about 20% of the isotope ^{10}B, which has a high enough cross section to reliably interact with thermal neutrons, thus preventing reactions with the fuel and decreasing the reactor power output. The same element is common in reactor control rods for this reason. Boric acid is therefore a common chemical in nuclear reactor installations, and it is likely that it, or compounds derived from it, will be present in case of an accident. If so, its interaction with the volatile fission products should be studied too.

This study aims to investigate the effects of boric acid on systems including iodine and tellurium, and simulating conditions similar to those expected during a severe nuclear accident. Specifically, the potential for an altered volatility of the fission products is of interest. In the case of tellurium, a recent study [3] investigated the change in tellurium oxidation behavior due to the presence of boric acid. This subject is further investigated here while also incorporating iodine, as well as cesium iodide.

2. Theory and Background

2.1. The volatile fission products

Iodine and cesium, and their interaction between each other are relatively well studied in the context of severe accidents. Some isotopes of particular interest are listed in Table 1. Especially iodine is a concern, as it contributed to a large part of the activity in the releases after both the Chernobyl and the Fukushima Accidents [4][5]. The decay of relevant Iodine isotopes gives rise to various xenon nuclides, which are in principle chemically inert.

Iodine melts at a temperature of 113.5 °C and boils at 184 °C at standard pressure. The transport of iodine in severe accidents is also rather unique, as it may be transported both as aerosol particles [6] or vapor form [7]. Aside from the noble gases, the other volatile fission products are typically transported as aerosol particles [7].

The most important cesium isotopes are listed in Table 1. Cesium melts at 28.5 °C and boils at 671 °C. The volatility and the long half-life of ^{137}Cs makes this isotope in particular a radio hazard with ramifications reaching far into the future.

Tellurium is yet another volatile fission product. It is a metalloid that melts at 450 °C and boils at 990 °C. It has a complex chemistry and can adopt several oxidation states, where the most common are -II, +II, +IV and +VI. From a radio hazard perspective, it is not as long-lasting as cesium (as seen in Table 1); the half-life of the most important tellurium isotope is 3.2 days. This makes it primarily a short-term concern. During the Chernobyl accident, the activity of released ^{132}Te was one of the highest for individual isotopes, and indeed higher than the activities of both ^{137}Cs and ^{134}Cs[8]. ^{132}Te decays into ^{132}I, which has a half-life of roughly 2.3 hours [9]. This means tellurium and iodine will coexist, and interactions between them warrant study. Furthermore, the release of tellurium results in a delayed release of iodine, which has implications for the iodine source term.

Table 1: Comparison of the releases between the Chernobyl Accident and the Fukushima-Daiichi Accident for selected Cs, I and Te isotopes. In all releases of the volatile fission products, the Chernobyl accident was significantly worse. Note that there are several studies of these releases, and that different studies report different releases.

Nuclide	Half-life[9]	Decay Product	Estimated released activity- Chernobyl [PBq] [10]	Estimated released activity - Fukushima-Daiichi [PBq][5]
^{129m}Te	33.6 days	^{129}I	240	15
^{132}Te	3.17 days	^{132}I/^{132m}I	1000	180
^{131}I	8.03 days	^{131}Xe/^{131m}Xe	1200-1700	150
^{133}I	20.83 hours	^{133}Xe/^{133m}Xe	2500	146
^{134}Cs	2.07 years	^{134}Ba	44-48	11.8
^{136}Cs	13.16 days	^{136}Ba	36	2.2-2.6
^{137}Cs	30.08 years	^{137}Ba/^{137m}Ba	74-85	12

2.2. Boron

Boron can be used as a means of reactor control due to the high nuclear cross section of the B^{10} nuclide with thermal neutrons. In pressurized water reactors (PWR) boron is an additive, where it is dissolved in the primary circuit water, often in the form of orthoboric acid (henceforth referred to as just “boric acid”). This affects the neutron economy in the reactor, allowing for an alternate method of controlling the reactor aside from the control rods[11][12].

Both of these uses make the element a likely component of the sump water in a severe accident, and warrants its interaction with various fission products be investigated. However, it should be noted that as Boric acid is present as an additive in the PWR primary circuit, its potential for interaction with fission products is not limited to the containment but may potentially also happen in the pressure vessel or the steam generator tubes. This, in turn, makes the relevant temperature range very large; from thousands of degrees in the reactor core, to potentially less than 100°C in the containment. The concentration of boric acid in the reactor tends to vary with the freshness of the fuel, with fresh fuel being the most reactive and thus necessitating the highest concentration of boric acid. As the fuel is being consumed, the concentration is lowered. Typical values across a fuel cycle vary between 1 g/l and few mg at the end of the cycle[11]. Relatively concentrated acid (2200 ppm) can also be injected into the circuit as part of an emergency shutdown, meaning that the concentration in the sump during or after a severe accident is likely even higher than that.

Boric acid is not stabile at elevated temperatures but undergoes a series of dehydration reactions, as described in the Reactions 1, 2, and 3 [13].

$$B(OH)_3 \leftrightharpoons HBO_2 + H_2O, \qquad T{\sim}142^oC \quad Reaction\ 1$$

$$4HBO_2 \leftrightharpoons H_2B_4O_7 + H_2O, \qquad T{\sim}167^oC \quad Reaction\ 2$$

$$H_2B_4O_7 \leftrightharpoons 2B_2O_3 + H_2O, \qquad T{\sim}327^oC \quad Reaction\ 3$$

This, however, implies the heating of the pure substance, rather than it being dissolved. Nevertheless, calculations performed with the NucleaToolbox and the database shows that vaporization of boric acid in Ar/H_2O forms $B_3O_6H_3$, and a calculation with FactSage 5.5 indicated gaseous release of $B_3O_3H_3$ between 127-727 °C [14].

The chemistry and physical characteristics of fission products have been investigated in projects such as VERCORS and PHÉBUS, and in smaller projects aimed at more specific questions. Furthermore, the data gained from the Chernobyl and Fukushima-Daiichi accidents themselves also provides insight, especially in the relative releases of the different fission products.

2.3. Interactions Between Cesium, Iodine, Boron and Tellurium

Iodine and cesium are both relatively well investigated, both in their interactions between one another as well as with boric acid.

According to NUREG-1465, as much as 95% of the Iodine which enters the containment from the reactor coolant system will be in the form of CsI [15]. If available, this species will react with molybdenum trioxide, forming cesium molybdates and gaseous iodine. This reaction is also affected by the partial pressure of oxygen in the system. The higher the oxygen partial pressure, the more gaseous iodine is formed [16]. This is postulated to be linked to the oxidation state of molybdenum, as the formation of I_2 only seems to happen when molybdenum is oxidized beyond oxidation state IV+ (beyond MoO_2)[17].

Similar results have been seen for the CsI- boric acid system, where the reactions described in Reactions 4 and 5 describe the resulting formation of gaseous iodine and cesium borates [14]. Note that "(c)" indicates a condensed state.

$$CsI(c) + B(OH)_3(g) \leftrightharpoons CsBO_2(c) + HI(g) + H_2O \quad Reaction\ 4$$

$$2HI(g) \leftrightharpoons I_2(g) + 2H_2(g) \quad Reaction\ 5$$

The process described by Reactions 4 and 5 has been shown to be very efficient at converting CsI into gaseous iodine. When vaporizing only CsI in inert argon gas with steam, only about 1% of the iodine found was in a gaseous form. Upon addition of boric acid, 94% of the iodine was in gaseous form [14]. Furthermore, the efficiency of this conversion was affected by the flow rate of the carrier gas, with a high flow rate lowering the conversion. Similarly, in the presence of water, reaction 6 and reaction 7 is a possibility which further influences the cesium and iodine chemistry.

$$CsI + H_2O \leftrightharpoons CsOH + HI \quad Reaction\ 6$$

$$CsOH + B(OH)_3 \leftrightharpoons CsBO_2 + 2H_2O \quad Reaction\ 7$$

Reaction 7, if it happens, consumes CsOH, thus driving reaction 6 further to the right. Equilibrium calculations performed indicate that the overall reaction of the reactions 6 and 7 becomes highly relevant at 1027 °C, whereas for 727 °C, the iodine will largely be present as CsI still, with only 18% being in the form of HI. This nevertheless implies that the presence of boric acid potentially can alter

the speciation of iodine and cesium drastically [18], all depending on the temperature and conditions.

Compared to cesium and iodine, tellurium is less studied, and its interactions with the other fission products is less rigorously investigated. It is released from the fuel at a similar time as cesium, so Cs-Te species may be formed in the reactor core during an accident. Examples would include Cs_2Te, or Cs_2TeO_3 [19]. The stability of these species in atmospheric conditions is uncertain, however, and their formation would be contested by species such as SnTe or even TeO_2, depending on the conditions. Tellurium and cesium did behave the same way after the Fukushima-Daiichi accident in that they tended to appear together as particulate species after the accident [20]. However, the ratio between them varied significantly, indicating that they did not necessarily form Cs-Te compounds, but rather that the particulates formed by them tended to behave in a similar manner.

Tellurium and iodine can react to form tellurium iodides. This is a class of compounds encompassing various ratios between tellurium and iodine, and what compound is formed will depend on the circumstances, as can be seen in the phase diagram presented in Figure 1. Note that the phase diagram only assumes two solid tellurium iodides; TeI and TeI_4, as it is assumed that these are the only compounds formed in the solid state [21]. However, in the vapor phase TeI_2 is also formed through decomposition of TeI_4 to TeI_2 and I_2. This is expected at temperatures above 500 °C, and further decomposition to the basic elements at temperatures above 600 °C[21].

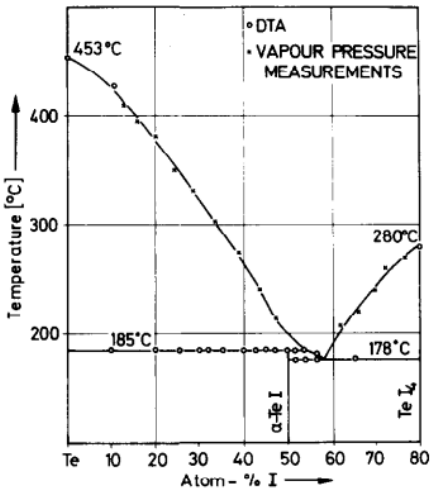

Figure 1: Phase diagram of the Te-I system [22, used with permission from the publisher].

Tellurium iodides have been studied in the context of severe accidents before by investigating the volatility of iodide in a tellurium matrix [23]. The investigated samples were produced by irradiating tellurium metal with neutrons, generating ^{131}I by decay from ^{131}Te. The ratio between the two elements therefore was in the range of 10^{10} atoms of Te per atom of I. Still, the results imply that tellurium (sub)iodides do form and remain volatile until temperatures of about 150-200 °C. This was determined by allowing the gaseous tellurium iodides to be carried down a furnace with a gradually decreasing temperature.

3. Methodology

A total of nine experiments were conducted at VTT, Espoo, Finland, as presented in Table 2. The analysis of the samples produced was then conducted in part at VTT, and in part at Chalmers University of Technology, Gothenburg, Sweden. The experiments are, in principle performed in a progressively more complex chemical environment, allowing the experiments to act as reference points to one another.

Table 2: Experimental conditions investigated throughout this work.

Experiment	Atmosphere	Injected through atomizer	Fission products
1.1	Oxidizing (Air)	-	I, Te
1.2	Oxidizing (Air)	$B(OH)_3$(aq)	I, Te
1.3	Oxidizing (Air)	$B(OH)_3$(aq), CsI (aq)	Te
2.1	Reducing (Ar/H_2)	-	I, Te
2.2	Reducing (Ar/H_2)	$B(OH)_3$(aq)	I, Te
2.3	Reducing (Ar/H_2)	$B(OH)_3$(aq), CsI (aq)	Te
3.1	Inert (N_2)	-	I, Te
3.2	Inert (N_2)	$B(OH)_3$(aq)	I, Te
3.3	Inert (N_2)	$B(OH)_3$(aq), CsI (aq)	Te,

The temperature in all these experiments was set to 650 °C, as to simulate the temperature in the primary circuit during a loss-of-coolant accident (LOCA). The three atmospheres used encompass both oxidizing and reducing conditions, both of which are theoretically possible during an accident, as well as an inert atmosphere.

Throughout all nine experiments, only singlets were performed, meaning uncertainties are impossible to determine.

3.1. Description of the experimental setup

The experiments were performed using two different setups. One setup was used to conduct the experiments X.1 and X.2 (where X is 1,2 or 3, indicating the respective experiment as seen in Table 2), whereas the final experiment (X.3) for each atmosphere, involving CsI, necessitated a slightly different setup. However, both setups draw inspiration from the setup previously used in the cooperation between VTT and Chalmers. Details can be found in [24], and the system used for the present study is schematically depicted in Figure 2. The three carrier gases consisted of synthetic air (21% O_2, 79% N_2) for the oxidizing conditions, N_2 for the inert conditions, and 5% H_2 by volume in argon, for the reducing conditions.

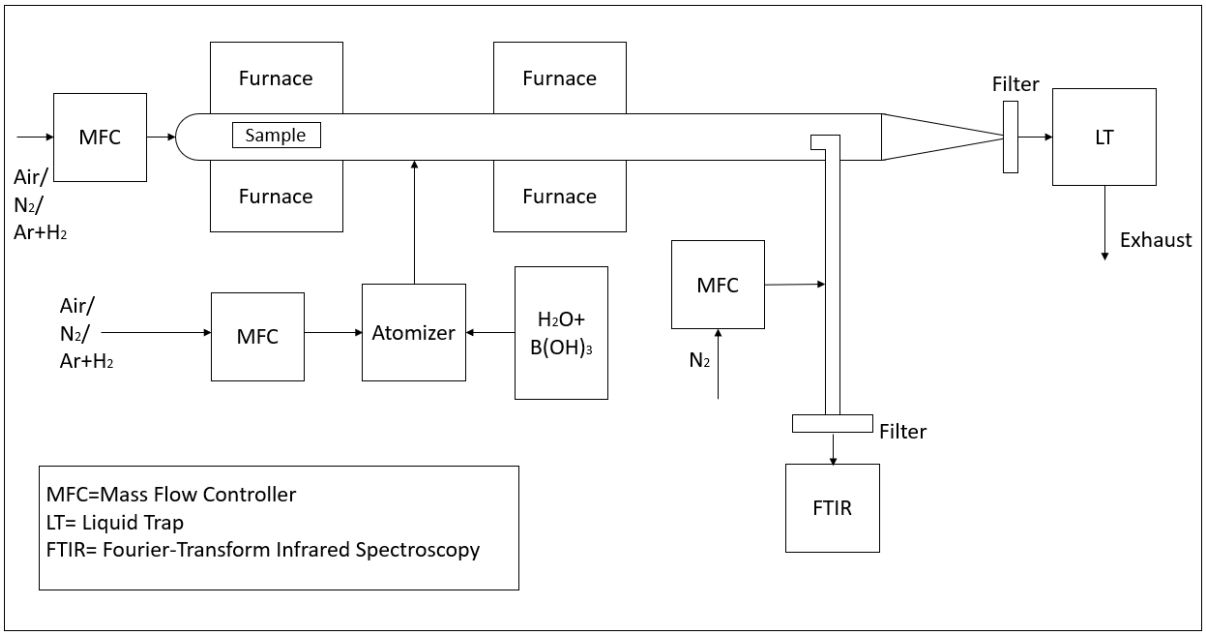

Figure 2: Schematic depiction of the experimental setup used for the majority of the experiments.

Two tubular flow furnaces (Entech Vecstar, VCTF 4) are connected in sequence with tubes made from stainless steel (AiSI 316L). These furnaces held the same temperature throughout the experiments and were the only points in the setup where the temperature was measured. The first furnace was loaded with a crucible of Al_2O_3 filled with 5 g Te (metal, Sigma-Aldrich, purity ≥99.997%) before each experiment. The temperature of this furnace was set to 540 °C, which is enough to volatize enough tellurium for the experiment. The gas flow through this furnace is in total 3 l/min for all three conditions. All the flows in use are controlled by mass-flow control units (Brooks S5851, Brooks® Instrument).

Between the two furnaces there is a connection where additional species can be introduced to the system. From here, iodine is added through one line. Iodine is supplied by placing pebbles of solid iodine in a sealed bottle, which in turn is heated in a water bath set to 65 °C. The flow through the iodine feed is 2 l/min, but before the flow enters the main line, 0.8 l/min is diverted through a liquid trap (100 ml 0.1 M NaOH) and sent to the exhaust. By analyzing the contents of the liquid trap, it is possible to determine the amount of iodine fed during the experiment.

Furthermore, an atomizer feeds a solution of 0.2 M Boric acid through this middle connection. The atomizer has a flow of 3 l/min. To ensure the total flow through the main line is similar for all conditions, whether or not boric acid is used, another line bypasses the atomizer and delivers a 3 l/min flow in the experiments which does not involve the boric acid solution.

Beyond the connective point, another furnace and tube is placed, identical to the first ones. The flow through this furnace contains all species in use for the experiment being run, and adds up to a total of 7.2 l/min. The temperature in this furnace was constant across all experiments and set to 650 °C.

Finally, beyond this furnace, 2.2 l/min of the flow is diverted to a secondary line which allows for an online FTIR measurement during the experiment. Before the FTIR, a filter (MilliPore, MitexTM PTFE, pore size 5 µm) is placed to catch any particulate matter.

The remaining 5 l/min of the flow is sent directly through an identical filter, after which it is diverted through a liquid trap (100 ml 0.1 M NaOH) to catch any species capable of penetrating the filter, especially volatile species. The outlet of the liquid trap is sent to the exhaust.

The first two (X.1 and X.2) experiments for each atmosphere run with this setup were all performed in an uninterrupted sequence. Each condition was run for 30 minutes. After 30 minutes, the gas flow after the second furnace was redirected to the exhaust while the filters and liquid traps were changed. This took about 10-15 minutes, after which the next experiment could be started by starting or stopping the relevant gas flows, without the need to the furnaces to cool down.

To accommodate for the use of CsI in the system, the setup has to be modified. These three conditions (experiments 1.3, 2.3 and 3.3) were run in the order of reducing, inert and oxidizing conditions. Each condition followed upon the other, and each condition lasted for 30 minutes. The method used has been described previously [24]. This means that 3 l/min carrier gas is added through the tellurium furnace, 3 l/min is added through the atomizer introducing $B(OH)_3$. To this liquid (200 ml 0.2 M $B(OH)_3$), 2 g CsI is added (for a concentration of 38.5 mM). Thus, CsI is added to the system via the same avenue as the $B(OH)_3$, after the tellurium has been volatized but before the reaction furnace at 650 °C. 2.2 l/min of the flow out from the reaction furnace is diverted to FTIR, whereas the last 5 l/min is directed through the filter and the liquid trap, as per the previous set of experiments. For the experiments with CsI, no iodine vapor was used.

Measurements of aerosol characteristics have been performed before on similar systems [3]. However, with iodine vapor present in the system, it was not suitable in this case. However, aerosol characteristics on tellurium and boric acid together have been investigated before [3] and the aerosols then formed had a count median diameter between 0.1 and 0.9 µm.

Both the filters were weighed with a bench scale to the precision of one tenth mg before and after the experiments to determine how much material was collected on them. The filters were then stored in petri-dishes wrapped in parafilm and stored in 8 °C for about 12 weeks.

3.2. ICP-MS

The liquid traps are analyzed with ICP-MS (inductively coupled plasma mass spectroscopy, Element 2, ThermoScientific) after the experiments to determine the concentration of Te, I, B and/or Cs. The detection limits for Tellurium (Te^{126}) was 0.006 ppb. The samples are diluted with 0.5 M HNO_3 (Suprapure) before the measurements, and 1 ppb Rh was used as internal standard.

3.3. XPS

XPS (X-ray photoelectron spectrometry) was conducted at Chalmers University of Technology, using the PHI5000 VersaProbe III- Scanning XPS Microprobe™ machine available. The x-ray source was a monochromatic AlKα source (1486 eV). Beam width was 100 µm, 25 W 15 kV, FWHM was 0.654 eV, determined from the $3d_{5/2}$ peak after measuring a sputter cleaned Ag sample. The system was aligned with Au (83.96 eV), Ag (368.21 eV) and Cu (932.62 eV), and the narrow scan measurements were aligned with the C1s signal at 284.6 eV before analysis. For XPS, the limit of detection depends on the element in question, and the sample matrix [25]. However, all expected elements could be determined for this study.

Survey scan proceeded from 0-1100 eV with a step size of 1 eV, and the narrow scans had a step-size of 0.1 eV. For the C1s signal the step size was 0.05 eV.

3.4. SEM

The filter samples were investigated with SEM, using the Quanta 200 FEG ESEM, manufactured by FEI, present at CMAL (Chalmers material analysis laboratory). Imaging was based on backscattered electrons and used a 15 kV voltage and a current at about 100 µA.

3.5. Production of Tellurium iodide

Samples of tellurium iodide were prepared using the stoichiometric ratio of 2 moles of iodine per 1 mole tellurium. The pure elements were mixed in an evacuated quartz ampule and heated to 400 °C. At this point the substance in the ampoule had melted into a solid lump, well below the melting point of tellurium at 449.5 °C. Note that TeI_2 does not exist in the solid phase[21].

4. Results

4.1. Chemical contents of the liquid traps

The chemical content of the liquid traps for each experimental condition for tellurium, boron, iodine and cesium are detailed in Table 3. These contents represent the gas-phase species in each condition.

Table 3: Contents of the liquid traps for the different experiments.

Experiment	Iodine content [mM]	Boron content [mM]	Tellurium content [µM]	Cesium content
1.1	5,67	0,46	0,27	-
1.2	6,02	2,26	7,44	-
1.3	0,19	0,34	2,35	Below detection limit
2.1	4,18	0,53	3,21	-
2.2	5,00	1,36	61,28	-
2.3	0,001	0,85	4,70	Below detection limit
3.1	1,30	0,25	0,04	-
3.2	5,28	2,29	117,12	-
3.3	0,13	0,92	5,49	Below detection limit

There are a few patterns that can be easily deduced: there is a consistent pattern in that the most trapped species is most often iodine, followed by boron, and tellurium is the species with the lowest concentration in the liquid trap. This holds for every experiment and is not surprising given that

iodine gas effectively penetrates the filter to the liquid trap, given that it should occur as a gaseous species. Compared to the filter weights (see section 4.3), it seems that the iodine tends to decrease as the number of particles increases, implying that there is a reaction between the particles and the iodine. The iodine content is plotted in Figure 3.

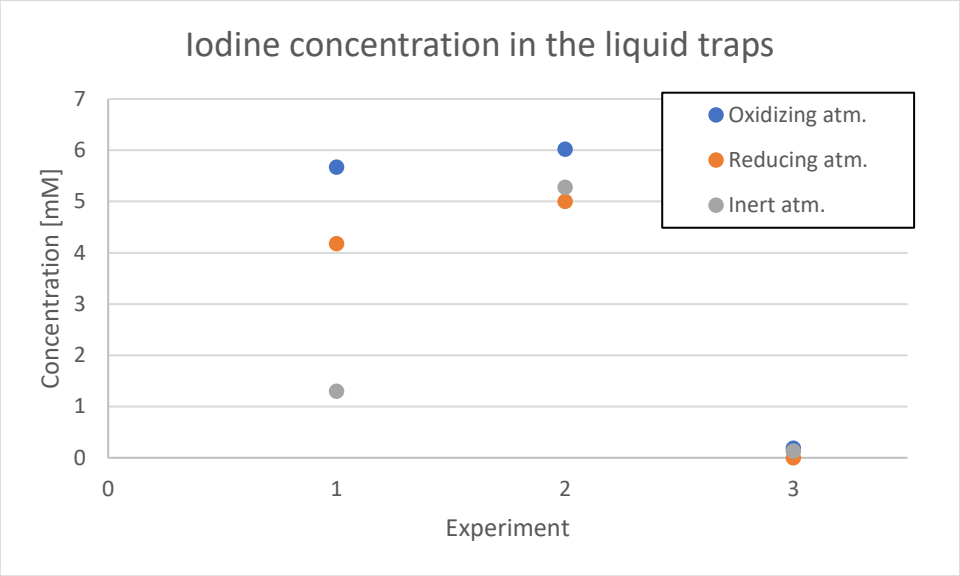

Figure 3: Iodine concentration in the respective liquid traps. "Experiment" refers to the different experiments 1-3, as labeled in Table 2.

Likewise, boric acid is volatile at these temperatures, though it tends to decompose to B_2O_3 which has a negligible vapor pressure even at significantly higher temperatures [26]. Indeed, no boric acid is added in the X.1-series of experiments, but the boron content is still consistently present. The theory is that this may be contamination from the borosilicate glass used for the liquid trap. The trap solution was 0.1 M NaOH, which does etch glass.

Tellurium only has a few volatile species under these conditions, aside from TeH_2, which would only be relevant in reducing conditions (experiments 2.1-2.3) and is still not very stable as the temperature falls from 650°C.

There is a sharp increase in tellurium and boron concentration in the liquid trap in all experiments X.2 compared to X.1. The difference between these is the addition of boric acid, which explains the boron increase. The reason for the tellurium increase is uncertain. The system including only tellurium and dissolved boric acid, in nearly identical conditions (similar setup, same temperature, same carrier gases etc.) have been investigated before [3]. However, no large increase in tellurium concentration could then be observed in the trap, other than for the reducing conditions at 650 °C. This increase was attributed to the formation of TeH_2.

With the experiments conducted, the increased volatility of the tellurium can be due to either the boric acid, water, or both. It is not possible to say which species is responsible based on this study. However, the hypothesis is that the increase is due to two effects working in tandem.

After the tellurium is volatilized in the furnace, the injection of water and iodine at the junction serves to lower the temperature of the gaseous tellurium. This causes the gas to condense into droplets. If there is iodine present in the system, the tellurium will form tellurium iodides, which are gaseous. As the temperature increases, these dissociate into gaseous tellurium and I_2. In this

hypothesis, the iodine serves to further disperse tellurium to a gaseous species. The gaseous tellurium further reacts with either the water, or the derivatives of boric acid and forms a volatile species. Potential species could be boranes (BH_3 or B_2H_6 for example), which are volatile and highly reactive species. However, this would only be remotely feasible in the reducing case, and since the synergistic effect is seen in all three investigated atmospheres, this explanation is not very likely. A potentially more appealing explanation would involve the formation of BI_3. It has a boiling point of 210°C and could, in theory, form in all three investigated conditions.

For the experiments using tellurium, CsI, and boric acid, there are few trends compared with earlier experiments. The tellurium content is in the same order of magnitude across all three atmospheres and generally low. Iodine likewise does not seem to be transported as a volatile species in these conditions, as evidenced by the iodine content being one or two magnitudes lower in these experiments compared to all other conditions. Likely this is because the iodine is added as ions dissolved in water for these experiments, rather than as a gas. Cesium is never detected in the liquid traps. The boron content, finally, is comparable to all other conditions.

4.2. Summary of the FTIR analysis

FTIR spectra failed to determine any volatile compounds with certainty. Commonly, the spectrum revealed water vapor, and, at times, isopropanol used to clean the system. Presumably, any volatile species is present in too low of a concentration to determine with FTIR. The limit of detection of the instrument was 1ppm. This would include TeH_2, which would be expected in some of the experiments performed in reducing conditions. Indeed, in a previous study, TeH_2 was also inferred from the liquid samples, but could still not be determined in the FTIR [3].

4.3. Filter Mass Analysis

The filters were weighted with a bench scale with the precision of one tenth milligram before and after the experiment. The change in the filter weights can be seen in Figure 4.

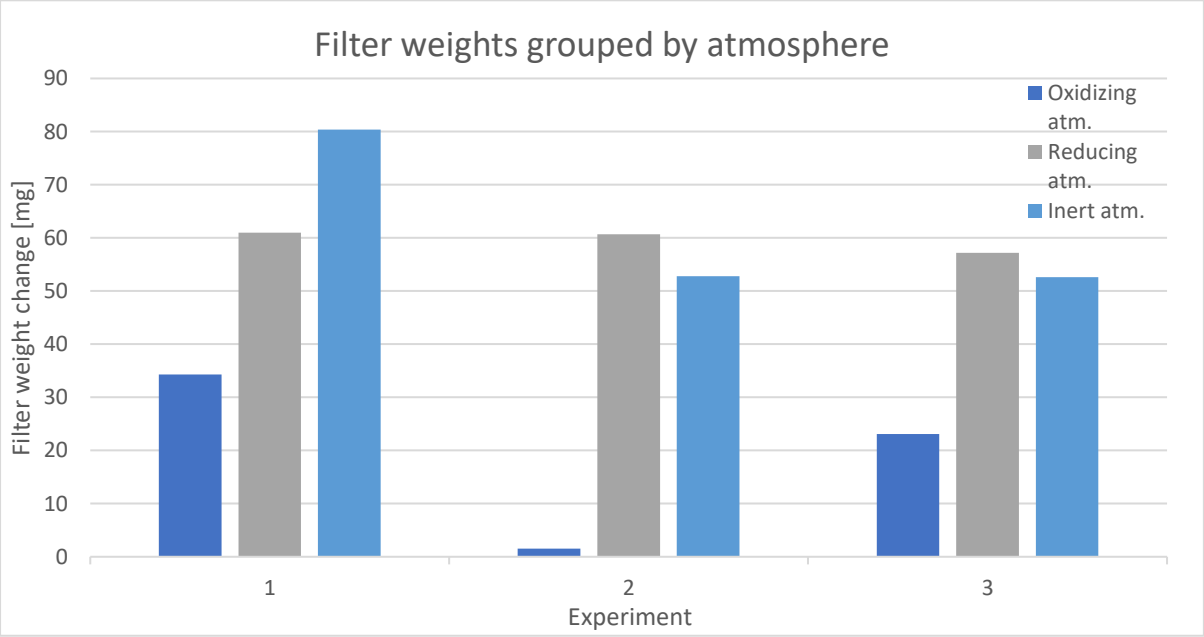

Figure 4: Increase in filter weight after the different experiments. 1- I+Te, 2- I+Te+$B(OH)_3$, 3- CsI+Te+ $B(OH)_3$

Across the range of filters there is one general remark to be made: the oxidizing atmosphere, no matter the other constituents of the system, makes for the least depositions on the filters. Largely, the low mass can be explained by the oxidation of the tellurium in the crucible into TeO_2, which is not volatile at these temperatures. However, the filter from experiment 1.1 (involving iodine and tellurium) and 1.3 (involving cesium iodine, tellurium and boric acid) do display a, for an oxidizing system, high filter weight, though not as high as in the cases of the reducing or inert atmospheres.

Looking at the corresponding XPS spectra for these two filters, the main element is tellurium. The signal for tellurium is made up of four different binding energies across the two experiments. For experiment 1.1 they are 576.4 eV and 577.9 eV, and for 1.3 they are 575.7 eV and 576.9 eV. This means three or potentially four tellurium compounds may exist in these samples. Comparing with the reference spectra of tellurium compounds suggests that the signals for 576.4 and 576.9 eV both belong to a tellurium oxide, either TeO_2 or TeO_3. The signal for 577.9 eV is less certain, but could be attributed either to TeO_3, or the hydrated form $Te(OH)_6$. All of these compounds are possible in an oxidized system, however none of these compounds should be volatile at this temperature, and there is no signal indicating the existence of metallic tellurium.

In the case of experiment 1.1, the reason for the large deposition on the filter could be due to a high availability of fresh, unoxidized tellurium in the precursor early in the experiment, contributing to a high deposition. The increased volatility at experiment 1.3 might be linked to the final signal, at 575.7 eV. The nature of that signal is uncertain and will be discussed further at the section dedicated to the XPS measurements, see chapter 4.5.

The reducing experiments all gave a very similar filter mass change after each experiment, implying that there is little change in the volatility of tellurium in either of these conditions. These are also the conditions where tellurium iodides were discovered (see further sections 4.4 and 4.5).

The mass of the filters for the various inert cases is mostly comparable to the reducing conditions, though no Tellurium iodide was discovered on these filters It could be noted, however, that the experiment with the very highest filter wight does correspond to the very lowest content of tellurium in the liquid trap. Clearly whatever species is responsible for this, it is not a very volatile one.

4.4. SEM analysis of the filters

A representative SEM-micrograph of the filters exposed to reducing atmosphere (experiment 2.2) can be seen in Figure 5.

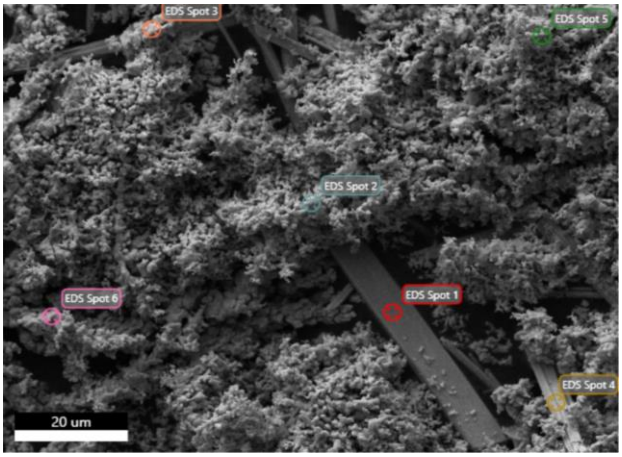

Figure 5: SEM micrograph of the filter exposed to Te, I, B(OH)3 and reducing atmosphere. Notice the large crystals embedded among the porous coverage.

The EDS- spectra for two representative spots (spot 1 and 2 in Figure 5) can be seen in Figure 6 and 7. The crystalline structures seen in Figure 5 appear to be composed of tellurium iodide. The ratio appears to be roughly equal, implying TeI as the species. The iodine appears to be collected in these crystals, as no EDS measurement other than those performed on the crystals show any iodine. The porous material appears to only contain tellurium.

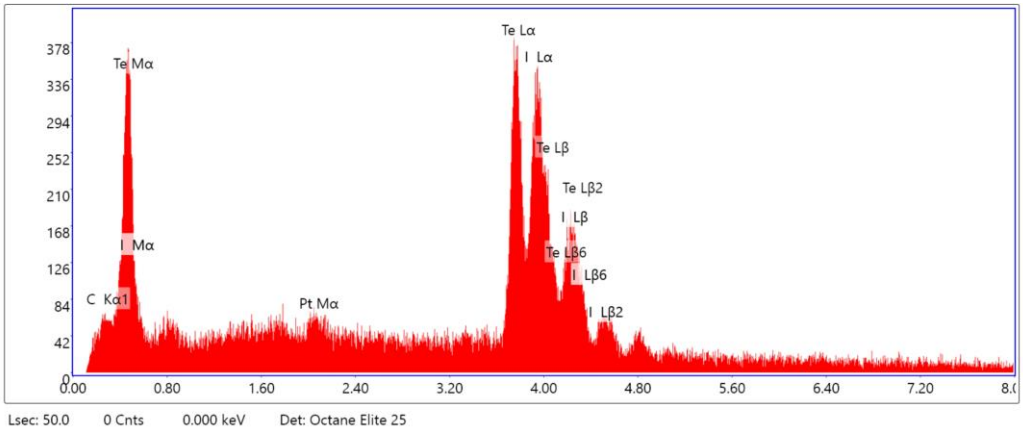

Figure 6: EDS-spectrum of spot 1 in Figure 5; the large crystal. The crystal surface seems to be composed of tellurium iodide, and quantification states the elements are present in roughly equal amounts.

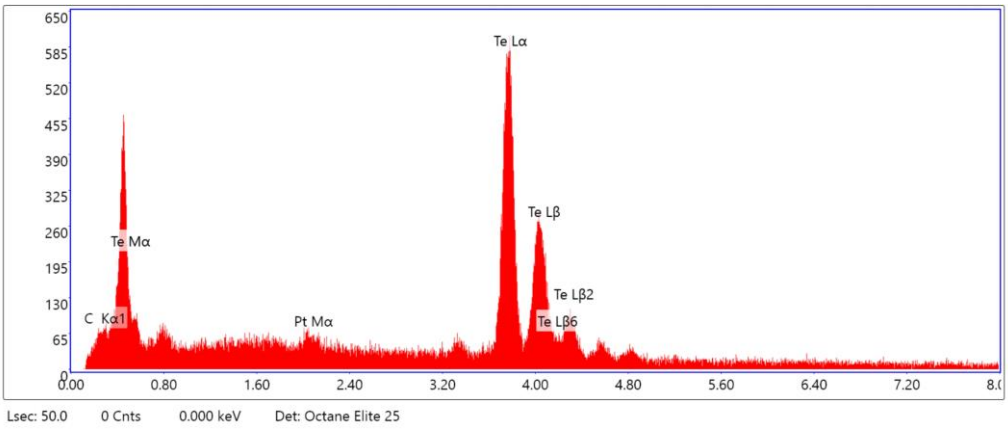

Figure 7: EDS-spectrum of spot 2 in Figure 5; the porous coverage. The porous coverage seems to be composed of practically pure tellurium metal. There is no indication of iodine in this spectrum.

A representative SEM-micrograph of the filters exposed to inert atmosphere (experiment 3.2) can be seen in Figure 8.

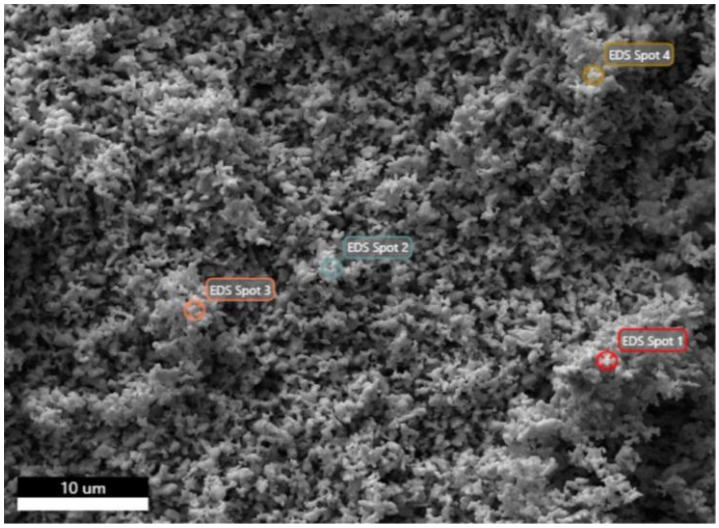

Figure 8: SEM micrograph of the filter exposed to Te, I, B(OH)3 and inert atmosphere.

The filter exposed to inert atmosphere contains only very few, significantly smaller crystals; mostly the surface is uniformly composed of tellurium, as determined by the EDS spectrum seen in Figure 9.

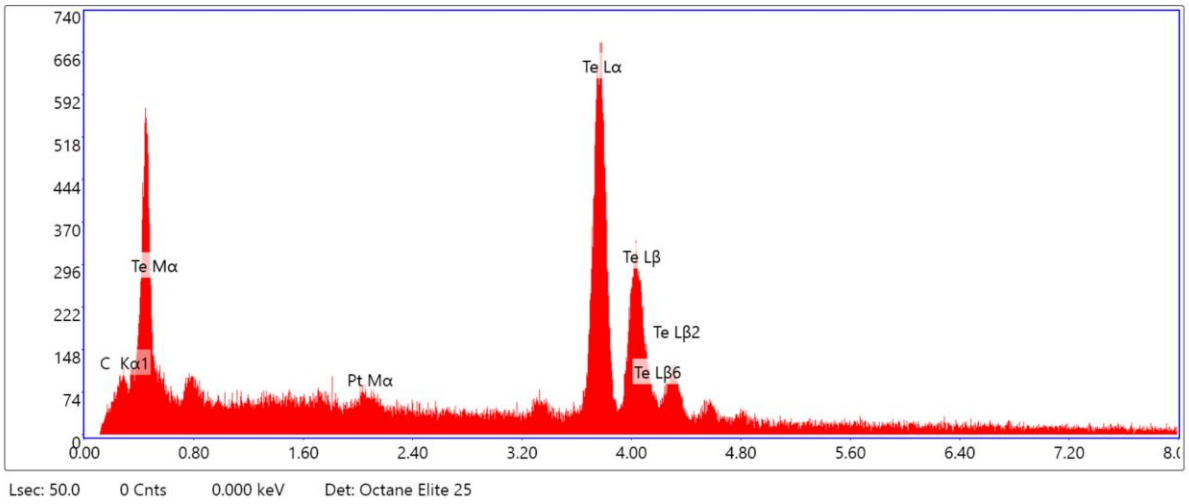

Figure 9: EDS-spectrum of spot 1 in Figure 8. The filter surface is mostly covered in a porous material that is composed of tellurium.

The lack of iodine deposition, and its prevalence in reducing conditions, implies that the formation of tellurium iodide is largely tied to the reducing atmosphere. A possibility is that the hydrogen telluride reacts with the iodine to form TeI_2. Another possibility is the formation of hydrogen iodide as an intermediary, and the direct reaction between molecular iodine and hydrogen is used industrially to produce HI. However, it then requires a palladium catalyst [27], which is not present in this study. The exact reaction method is not possible to determine from these experiments.

The tellurium aerosols appear similar in all cases as submicron, spherical particles. This description and the size line up with what was discovered when investigating the effect of boric acid on just tellurium [3]. According to the XPS analysis, those particles are also mostly tellurium, and the size is similar to what can be seen in the micrographs in Figures 5 and 8. This could be expected, as these spherical aerosols seem to consist of almost pure tellurium, which was also seen in the study without iodine [3]. It appears that the presence of iodine does not change the aerosol formation very much, aside from the presence of tellurium iodide in some cases.

For the oxidizing atmosphere, the deposited particles were strongly oxidized, and the electrical conductivity was poor. No conclusions could be drawn from those images.

4.5. XPS Analysis of Filters

For each of the twelve experiments, a survey spectrum from the particle deposition on each filter is collected to get an idea of the relative surface abundances of the different elements. Furthermore, the signal of each individual element is investigated with a finer resolution to gain insights in chemical shifts exhibited by each element which, in turn, helps with identification of the chemical state of the elements. The signal peak(s) for each element and each experimental condition are summarized in Table 4.

Table 4: Peak XPS signal position for each element and each experimental condition.

Experiment	Tellurium signal peak, $3d_{5/2}$ [eV]	Iodine signal peak, $3d_{5/2}$ [eV]	Cesium signal peak $3d_{5/2}$ [eV]
1.1	576,4 577,9	618,9 620,3	-
2.1	576,5	619,2	-
3.1	573,8 576,8	618,6 619,9	-
1.2	576,4	618,8 620,1	-
2.2	574,0	619,5	-
3.2	573,7	619,5	-
1.3	575,7 576,9	618,3 619,6	723,9 725,3
2.3	571,8 573,5 576,0	617,5 619,0 620,1	723,2 724,7
3.3	573,6 576,5	619,4 620,5	725,2

There were also spectra for the boron content in the conditions where boron is relevant, but in general the signal was very weak and difficult to interpret with certainty. Literature seems to suggest transport mainly as boric acid or the trimer of metaboric acid ($H_3B_3O_6$) in temperatures between 127 ^oC and 727 ^oC [14].

For the tellurium speciation, there are four to five broad classes of signals, all of which can be attributed to different compounds depending on the present conditions.

The experiment using Te, CsI and $B(OH)_3$ in a reducing atmosphere shows a tellurium signal at the energy 571.8 eV. This is the only time this signal is detected, and it is tentatively attributed to some form of cesium telluride. Depending on the ratio of Cs to Te, the signal varies between 572.4-572.7 for the Te-Cs bond[28]. This range of tellurium signals typically includes metal tellurides, and there should be no other metals available in the system (unless the furnace tube itself is corroded, which there was no sign of). The fact that the only time this signal is observed is in a system which includes cesium iodide also lends some credence to the theory.

The signals between 576.3 and 576.9 is attributed to TeO_2 [29], alternatively TeO_3 [30]. The signals for these compounds are close to one another, and determining one from the other with certainty is difficult. However, as the sample surfaces were likely oxidized to some degree during storage, the formation of these compounds is likely. There are also a pair of signals at the lower end of this range, at 575,7 and 576,0 eV. These signals are comparatively low for tellurium oxides, though not unreasonable [31]. They are tentatively assumed to be TeO_2. Finally, the high energy signal in experiment 1.1 (oxidizing condition, I and Te) at 577.9 eV is higher than both TeO_2 and TeO_3. This signal is beyond what tellurium compounds should show in XPS, and no conclusive answer can be given about its nature. It is tentatively assumed to indicate Te(OH)6, a hydrated form of TeO_3 which should have a slightly increased energy compared to the non-hydrated form. However, its energy

should be closer to 577 than 578 [31]. An example of spectra (survey spectra and detailed spectra of tellurium and iodine) for the oxidizing conditions can be seen in Figure 10.

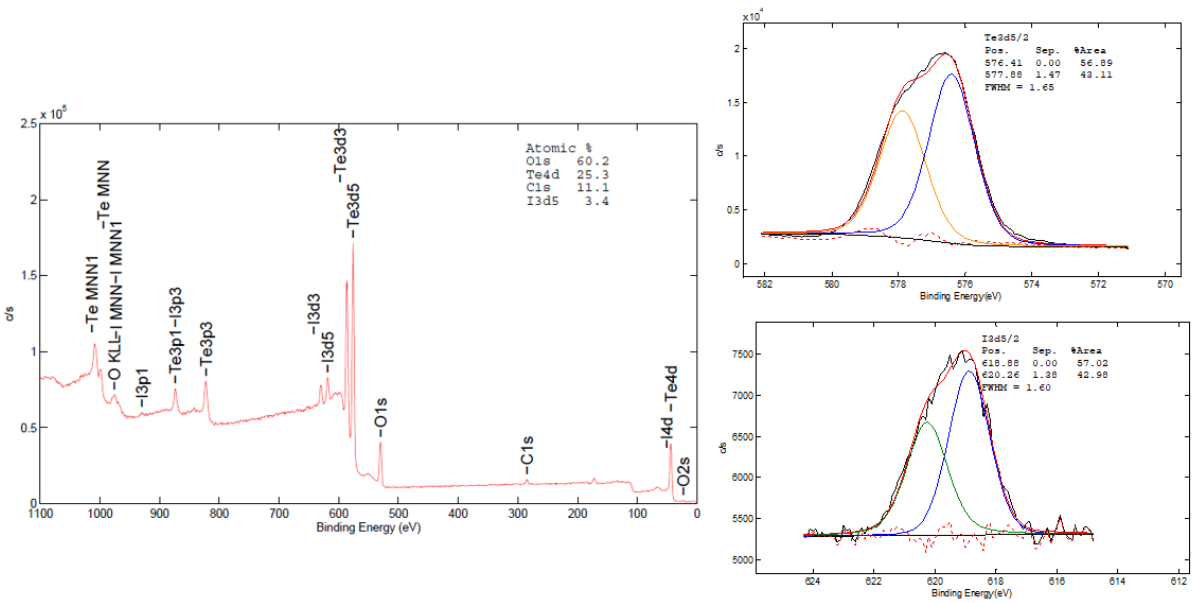

Figure 10: Survey spectrum and elemental abundance of the filter exposed to oxidizing conditions and Te and I. Also, the spectrum for the tellurium (top) and iodine (bottom).

Notice that the ratio of tellurium to oxygen is slightly above 1:2, potentially implying oxidation beyond TeO_2.

Finally, for the signals between 573.5 and 574.0, there are two species with similar signals. By comparing the values to literature, this can be metallic tellurium, as the values matches well; 573.54 eV [29] and 572.9 [30] respectively.

The alternative is that these signals are due to tellurium iodide. To investigate this possibility, a sample of tellurium iodide was prepared in-house and measured with PXRD. The resulting spectrum for the compound can be seen in Figure 11. It matches well with the reference spectrum, TeI_4 (blue peaks), though some contaminant seems to be present as well. Most likely this is due to a different stoichiometry of tellurium and iodine in different parts of the sample (potentially Te-I). As the sample was formed as a solid lump, iodine and tellurium ratio varied with location during formation.

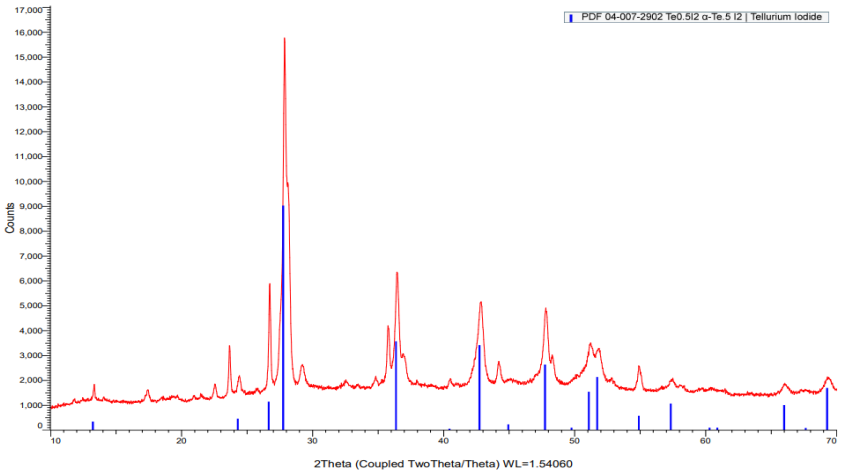

Figure 11: PXRD of the in-house produced sample for Tellurium Iodide (red line). The blue lines indicate the reference spectrum, TeI_4.

This sample was measured with XPS. However, the elemental composition reveals the ratio of tellurium to iodine being almost 4:1 on the sample surface. The resulting spectrum for that sample can be seen in Figure 12.

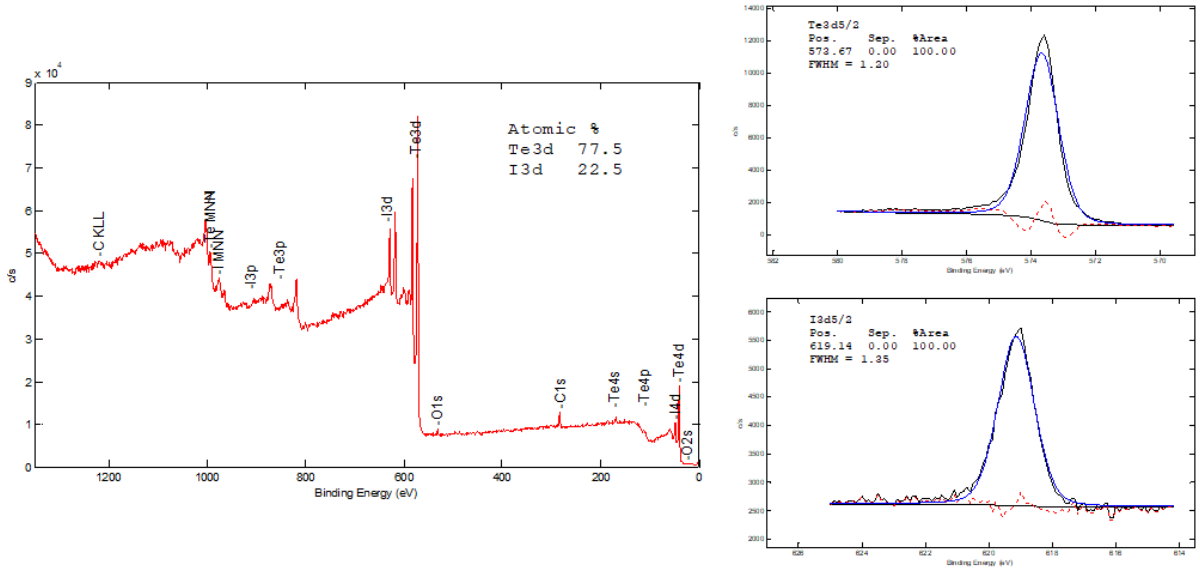

Figure 12: Survey spectrum and elemental abundance of the Te_4I prepared in-house. Also, the spectrum for the tellurium (top) and iodine (bottom).

The compound gave a tellurium signal at 573.7 eV, matching very well with the signals 573.5-574 eV.

Based on these results, the hypothesis that tellurium iodide can be difficult to differentiate from tellurium metal is strengthened. Clearly, if the iodine content is relatively low, the XPS signals will overlap. However, as tellurium iodide is confirmed in the samples using SEM-EDX, and can also be implied from XPS, it appears that this compound has formed.

The survey spectra, and the relevant spectra for iodine and tellurium, are included for the reducing condition in Figure 13, and for inert conditions in Figure 14.

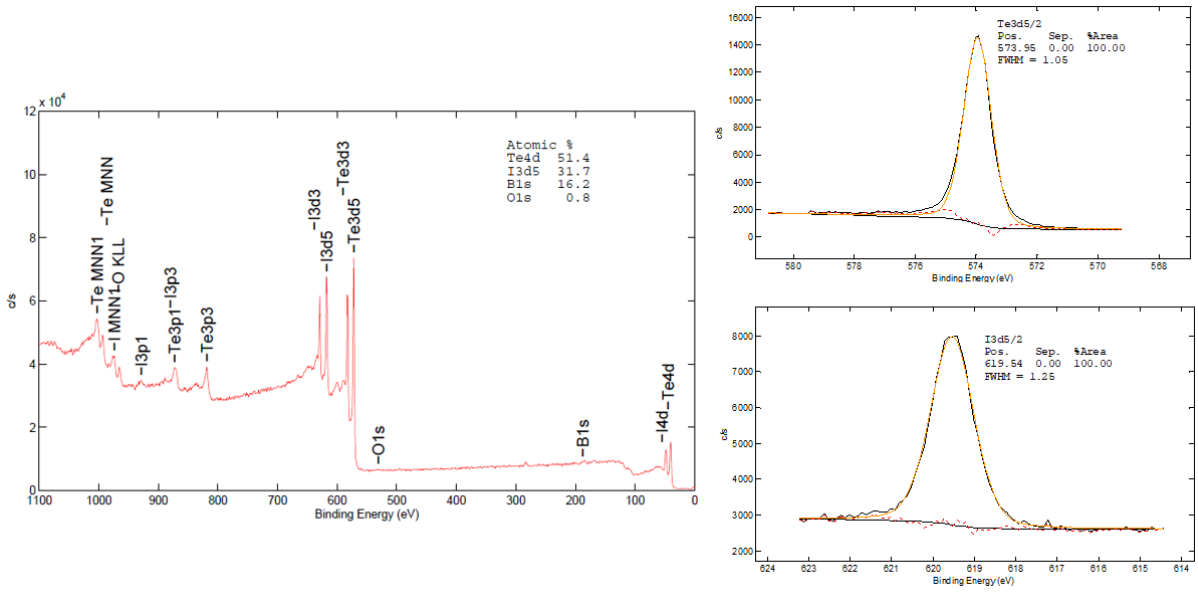

Figure 13: Survey spectrum and elemental abundance of the filter exposed to reducing conditions and Te, I, and B(OH)3. Also, the spectrum for the tellurium (top) and iodine (bottom).

The survey spectra implies that the behavior of iodine is different in reducing conditions compared to the inert (and oxidizing) case, as the iodine fraction is significantly higher in the reducing case; 31% compared to 4% in the inert case. The oxidizing case (not shown) had an iodine content of 0.7%.

Comparing the XPS signals with the EDS speciation (see section 4.4.) implies that both metallic tellurium and tellurium iodide are present in different samples. Samples exposed to inert atmosphere have mostly metallic tellurium and very little tellurium iodide, whereas systems exposed to reducing conditions had rather prominent tellurium iodide crystals deposited on them.

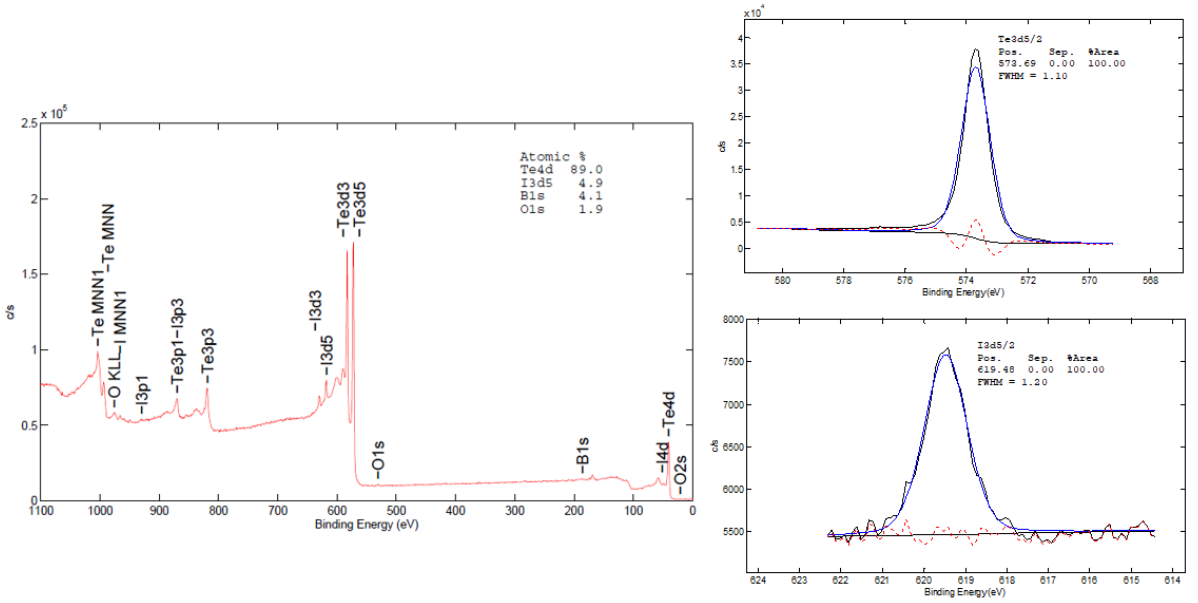

Figure 14: Survey spectrum and elemental abundance of the filter exposed to inert conditions and Te, I, and B(OH)3. Also the spectrum for the tellurium (top) and iodine (bottom).

XPS signals for iodine can roughly be divided into three classes. The most common signal, which is present in almost every sample (except for experiment 1.3, oxidizing atmosphere, with Te, CsI and $B(OH)_3$ present) varies between the energies 618.6- 619.5 eV. The tellurium iodide prepared in-house displayed an iodine signal of 619.1 eV, matching well. However, it does overlap to some degree with the expected signal for I_2, which ought to have a signal at 619.9 [31]. It is possible that both species are present for different experimental conditions. From the survey scans, tellurium iodide may be the reason for the high iodine content in the reducing case with Te, I, and $B(OH)_3$, as seen in Figure 13. According to the literature [21], [23] tellurium iodide would also be volatile at the temperature of 650°C, but may condense as the temperature falls and be collected on the filter.

The fact that the detailed XPS scans in Figure 13 and 14 implies the same compounds for tellurium and iodine in both inert and reducing conditions is worth discussing. As the amount of iodine in the inert case is very low, presumably the majority of the tellurium is in the form of tellurium metal in that case. As has been noted, tellurium iodide and tellurium metal are similar in XPS.

The experiments involving cesium iodide in both reducing and oxidizing conditions each display relatively low signal at 617.5 and 618.3 eV respectively. These signals are assumed to correspond to CsI [32], though they are admittedly slightly low compared to the literature. Several samples also display signals around 619.6 eV up to 620.3 eV, which corresponds reasonably well to I_2.

Cesium, finally, displays two classes of signals, 723.2-723.9 eV and 724.7-725.3 eV. For the second range, a certain answer is not possible with XPS alone, as there are two possibilities. As suggested above, some form of cesium telluride would fit the signal, as its reported value is around 524.6-526.4 eV[28], again depending on the Cs-Te ratio. Lower amounts of Cs give rise to lower energy values. The other alternative is CsOH, with an energy at 724.5 eV [33].

The first class of signals is attributed to CsI, matching well with some of the literature values [34]. Note, however, that the reported signal for iodine in this paper differs significantly from the signal reported in [32] for the same compound.

5. Conclusions

The filter weights and the liquid trap chemical contents both indicate that the presence of oxygen serves to prevent tellurium volatilization at 650°C, due to oxidation of tellurium. The filter weights at this atmosphere are consistently the lowest, and the tellurium content of the liquid traps are also very low if not the lowest for any given result.

It is difficult to determine tellurium metal from tellurium iodide in the XPS analysis. However, from the SEM micrographs, the presence of a tellurium-iodide species is confirmed, and XPS analysis of an in-house produced sample of tellurium iodide also lends credence to this confirmation. It seems like tellurium iodide(s) can form and remain stable for some time under these conditions, as evidenced by the SEM-EDX analysis.

The liquid trap analysis reveals an increase in tellurium and boron concentration when iodine, tellurium, and boric acid all are used together. However, there is no significant increase in the iodine concentration. This pattern is true for every investigated atmosphere. The boron increases also be explained by the addition of boric acid in this experiment, though the same increase in boron concentration would then be expected in the CsI-$B(OH)_3$-Te experimental series, which did not occur. This may imply the formation of a volatile boron-tellurium compound, but this is unprecedented in the literature, and could not be conclusively determined from the XPS analysis. The increase is also not seen upon investigating tellurium with just boric acid [3]. A possibility is the

formation of BI_3, which forms a volatile complex with tellurium, but the exact species and mechanism cannot be deduced from these experiments alone.

The tellurium and boron increase observed in this study appears dependent on iodine, tellurium, and boron all being present together, and can be of potential interest for severe accident analysis. Due to ^{132}Te decaying into $^{132(m)}I$ (with a half-life of 3.17 days), tellurium and iodine will always be present together in an accident sequence. Addition of boric acid to such a system, days or weeks after the accident, may potentially cause volatilization of the tellurium.

6. Acknowledgements

The authors acknowledge the Nordic nuclear safety research organization (NKS) for partially funding the project, as well as the Chalmers laboratory for material analysis CMAL for assistance with PXRD and SEM.

Special thanks also to Eric Tam for his assistance with the XPS analysis, and to Mark R.StJ. Foreman for his assistance with preparing TeI_4.

7. Declaration of competing interests

The authors declare that they have no known competing financial interests or personal relationships that could have appeared to influence the work reported in this paper.

8. References

[1] V.Kazakov, E. Demidchik, L. Astakhova, *Thyroid cancer after Chernobyl*, *Nature*, 359, 21, 1992, https://doi.org/10.1038/359021a0, retrieved 2023-05-23.

[2] G. Brillant, C. Machetto, W. Plumecocq, *Fission product release from nuclear fuel I. Physical modelling in the ASTEC code, Annals of Nuclear Energy*, 61 (2013) 88–95, http://dx.doi.org/10.1016/j.anucene.2013.03.022, retrieved 2021-11-29

[3] F. Börjesson Sandén, A-E. Pasi, T. Kärkelä, T. Kajolinna, C. Ekberg, *Effects of boric acid on volatile tellurium in severe accident conditions*, Annals on Nuclear Energy, 200, (2024), https://doi.org/10.1016/j.anucene.2024.110412

[4] N. Kinoshita, K. Sueki, K. Sasa, J. Kitagawa, S. Ikarashi, T. Nishimura, Y. Wong, Y. Satou, K. Handa, T. Takahashi, M. Sato, T. Yamagata, *Assessment of individual radionuclide distributions from the Fukushima nuclear accident covering central-east Japan*, *Proceedings of the National Academy of Sciences of the United States of America*, Vol 108, No 49, 2011, pages 19526-19529, DOI https://www.jstor.org/stable/23059527, retrieved 2021-11-25.

[5] G. Steinhauser, A. Brandl, T. E. Johnson, *Comparison of the Chernobyl and Fukushima nuclear accidents: A review of the environmental impacts*, *Science of the Total Environment*, 470-471 (2014), pages 800-817, DOI http://dx.doi.org/10.1016/j.scitotenv.2013.10.029 retrieved 2021-11-25

[6] A.-C. Grégorie, T. Haste, *Material Release from the bundle in Phébus FP*, *Annals of Nuclear Energy*, 61, 2013, http://dx.doi.org/10.1016/j.anucene.2013.02.037, retrieved 2021-11-29

[7] T. Haste, F. Payot, P.D.W.Bottomley, *Transport and deposition in the Phébus FP circuit*, *Annals of Nuclear Energy*, 61, 2013, http://dx.doi.org/10.1016/j.anucene.2012.10.032, retrieved 2021-11-29

[8] *United Nations Scientific Committee in the Effects of Atomic Radiation, 1988 Report to the General Assembly, with Annexes- Annex D, exposures from the Chernobyl Accident*, UNSCEAR, 1988, retrieved 2023-09-18, ISBN: 92-1- 142143-8

[9] J. Magill, G. Pfennig, R.Dreher, Z. Sóti, *Karlsruher Nuklidkarte- Chart of the Nuclides 9:th edition*, Nucleonica GmbH, 2015, ISBN 978-3-943868-04-3.

[10] United Nations Scientific Committee on the Effects of Atomic Radiation, *UNSCEAR 2000 Report to the General Assembly, with Scientific Annexes- Volume II: effects*, *Annex J: Exposures and effects of the Chernobyl accident*, 2000, ISBN: 92-1-142238-8

[11] K. H. Neeb, *The Radiochemistry of Nuclear Power Plants With Light Water Reactors*, Walter de Gruyter, 1997, pages 27-42, retrieved 2021-08-11

[12] T.J. Connolly, *Foundations of Nuclear Engineering*, published by John Wiley & sons Inc., printed in the US, 1978, pages 207-292

[13] G. Kaur, S. Kainth, R. Kumar, P. Sharma, O.P. Pandey, *Reaction kinetics during non-isothermal solid-state synthesis of boron trioxide via boric acid dehydration*, *Reaction Kinetiks, Mechanisms and Catalysis*, 2021, 134, 347-359, https://doi.org/10.1007/s11144-021-02084-8, retrieved 2023-04-27

[14] M. Gouëllo, J. Hokkinen, E. Suzuki, N. Horiguchi, M. Barrachin, F. Cousin, *Interaction between caesium iodide particles and gaseous boric acid in a flowing system through a thermal*

gradient tube (1030 K–450 K) and analysis with ASTEC/SOPHAEROS , *Progress in Nuclear Energy*, 138, 2021,
https://doi.org/10.1016/j.pnucene.2021.103818, retrieved 2022-08-19

[15] L. Soffer, S.B. Burson, C.M. Ferrell, R.Y. Lee, J.N. Ridgely, *Accident Source Terms for Light-Water Nuclear Power Plants- Final Report*, U.S. Nuclear Regulatory Commission (NRC)- Office of Nuclear Regulatory Research, 1995, retrieved 2023-05-31, Accident Source Terms For Light-Water Nuclear Power Plants (NUREG-1465) | NRC.gov

[16] M. Gouëllo, J. Hokkinen, T. Kärkelä, *Advances in the understanding of molybdenum effect on iodine and caesium reactivity in condensed phase in the primary circuit in nuclear severe accident conditions*, *Nuclear Engineering and Technology*, 52, 2020, 1638-1649, https://doi.org/10.1016/j.net.2020.01.029, retrieved 2023-05-11

[17] S. Sunder, *The relationship between molybdenum oxidation state and iodine volatility in nuclear fuel*, Nuclear Technology, 144, 2003, 259-273, https://doi.org/10.13182/NT03-A3443, retrieved 2023-05-31

[18] T.S. Kress, E.C. Beahm, C.F. Weber, G.W. Parker, *Fission Product Transport Behaviour*, *Nuclear Technology*, 1010:3, 262-269, 1993, DOI: 10.13182/NT93-A34789, Retrieved 2022-08-26

[19] J.McFarlane, J.C.LeBlanc*, Fission product Tellurium and Cesium Telluride Chemistry Revisited*, No. AECL-11333, Atomic Enegry of Canada Ltd., 1996, retrieved 2021-10-11

[20] R.S. Dickson, G.A. Glowa, *Tellurium behaviour in the Fukushima Dai-ichi Nuclear Power Plant accident*, *Journal of Environmental Radioactivity*, 2019, 204, 49–65, https://doi.org/10.1016/j.jenvrad.2019.03.024, retrieved 2021-10-08

[21] R. Kniep, A. Rabenau, *Subhalides of tellurium*, *Physical and Inorganic Chemistry*, Topics in Current Chemistry, vol 111, 1983, Springer, Berlin, Heidelberg, https://doi.org/10.1007/3-540-12065-3_3, retrieved 2023-12-21

[22] R. Kniep, A. Rabenau, H. Rau, Phase relationships in the Te-TeI4 system, Journal of the Less Common Metals, Vol. 35, 2, 1974, Pages 325-329, https://doi.org/10.1016/0022-5088(74)90244-6, retrieved 2023-12-21

[23] E. Karlsson, J. Neuhausen, R. Eichler, A. Vögele, A. Türler, *Adsorption properties of iodine on fused silica surfaces when evaporated from tellurium in various atmospheres*, *Journal of Radioanalytical and Nuclear Chemistry,* 326, pages 711–718, 2020, https://doi.org/10.1007/s10967-020-07326-y, retrieved 2023-12-21

[24] A-E. Pasi, T. Kärkelä, F.B. Sandén, U. Tapper, T. Kajolinna, C. Ekberg, *Gas phase interactions between tellurium and organic material in severe nuclear accident scenarios*, *Annals of Nuclear Energy,* vol. 197, 2024, https://doi.org/10.1016/j.anucene.2023.110247, retrieved 2023-12-01

[25] F. A. Stevie, C.L. Donley, *Introduction to X-ray Photoelectron Spectroscopy, Journal of Vacuum Science & Technology A*, vol. 38, 6, 2020, DOI: 10.1116/6.0000412, retrieved 2023-011-08

[26] S.S. Cole, N.W. Taylor, *The System Na_2O-B_2O_3 IV Vapor pressures of boric oxide, sodium metaborate and, and sodium diborate between 1150°C and 1400°C*, *Journal of the American ceramic society*, vol 18, 1935, pages 82-85, retrieved 2023-12-01.

[27] T. Kaiho (editor and author), *Inorganic Iodides. In Iodine Chemistry and Applications*, Published by John Wiely & sons Inc. 2014, https://doi.org/10.1002/9781118909911.ch5

[28] L. Soriano, L. Galan, R. Rueda, *An XPS study of Cs_2Te photocathode materials*, *Surface and interface analysis*, vol 16, 1-12, 1990, pages 193-198, **https://doi.org/10.1002/sia.740160138**, retrieved 2023-10-04

[29] A.J. Ricco, H.S. White, H.S. Wrighton, *X-ray photoelectron and Auger electron spectroscopic study of the CdTe surface resulting from various surface pretreatments: Correlation of photoelectrochemical and capacitance-potential behavior with surface chemical composition*, *Journal of vacuum science and technology A*, vol 2, 2, 1984, pages 1910-1915, retrieved 19-09-2023, https://doi.org/10.1116/1.572547

[30] W.E. Swartz Jr., K.J. Wynne, D.M. Hercules, *X-ray photoelectron spectroscopic investigation of group VI-A elements*, *Analytical Chemistry*, vol. 43, 13, 1971, pages 1884-1887, https://doi.org/10.1021/ac60307a044, retrieved 2023-09-19

[31] J.F. Moulder, W.F. Stickle, P.E. Sobol, K.D. Bomben, Handbook of X-ray Photoelectron Spectroscopy, Physical Electronics Inc., 1995, pages 130-131.

[32] P.M.A. Sherwood, *X-ray photoelectron spectroscopic studies of some iodine compounds, Journal of the chemical society*, *Faraday Transactions 2: Molecular and Chemical Physics*, vol. 72, 1976, pages 1805-1820, retrieved 2023-10-04, **https://doi.org/10.1039/F29767201805**

[33] H. Mores, J.G. Dillard, H. Klewe-Nibenius, G. Kirch, G. Pfennig, H.J. Ache*, XPS study of Iodine released in core melting experiments*, Surface and Interface analysis, vol. 7, 1, 1985, pages 22-28, https://doi.org/10.1002/sia.740070106

[34] W.E. Morgan, J.R. van Wazer, W.J. Stec, *Inner-orbital photoelectron spectroscopy of the alkali metal halides, perchlorates, phosphates, and pyrophosphates*, *Journal of the American Chemical Society*, vol. 95, 3, 1973, pages 751-755, retrieved 2023-10-04, https://doi.org/10.1021/ja00784a018